Universidad de Valladolid

ESCUELA DE INGENIERÍAS INDUSTRIALES

MÁSTER EN INGENIERÍA AMBIENTAL

# MASTER EN INGENIERÍA AMBIENTAL
## ESCUELA DE INGENIERÍAS INDUSTRIALES
## UNIVERSIDAD DE VALLADOLID

**TRABAJO FIN DE MÁSTER**

# Coupling photosynthetic biogas upgrading with the astaxanthin production using *Neochloris* sp.


Autor: Masashi Fujii

Tutor: Prof. Dr. Raul Muñoz Torre

Assistant Prof. Dr. Viktoriia Komarysta


Valladolid, July 12th

**Abstract**

The feasibility of coupling photosynthetic biogas upgrading with astaxanthin production by *Neochloris* sp. using real centrate as a feedstock was herein evaluated. To maximize astaxanthin production, this study focused on optimizing the cultivation conditions such as light intensity, culture medium, and composition of biogas. A light intensity of 300 μmol $m^{-2}$ $s^{-1}$ showed the highest specific growth rate (0.34 $d^{-1}$) and total suspended solid of biomass (0.33±0.03 g $L^{-1}$) of microalgae compared to other light intensity (0, 100, 500, 800 μmol $m^{-2}$ $s^{-1}$). When the headspace in the bottles was filled with air, mineral salt medium showed higher growth (0.78±0.007 g $L^{-1}$) than other medium conditions (10% diluted centrate from domestic wastewater, 10% diluted centrate adjusted initial pH of 7, and 10% diluted centrate with activated sludge aliquot). On the other hand, when biogas was injected into the headspace in the bottles, 10% diluted centrate showed a higher specific growth rate (0.58-1.1 $d^{-1}$) and TSS (2.57±0.92~6.98±0.029 g $L^{-1}$) because pH control by $CO_2$ dissolution prevented growth inhibition by free ammonia. In terms of biogas upgrading, $CO_2$ of the headspace in the bottles was removed by 82.8-99.8% and decarbonization of biogas was achieved. Interestingly, biogas containing 600 ppm $H_2S$ revealed a two-fold higher biomass yield than biogas without $H_2S$. When 5000 ppm of $H_2S$, growth inhibition occurred, but addition of activated sludge aliquot was effective to remove $H_2S$ by sulfur oxidizing bacteria, and microalgae grew (4.36±0.057 g $L^{-1}$). Thus, this study indicated that *Neochloris* sp. could validated the proof of concept with biogas containing 600 ppm $H_2S$. Comparison of the maximum biomass yield with different dilution centrate under a headspace of biogas with 600 ppm $H_2S$ showed no significant differences. Astaxanthin yield were 0.072% of dry biomass (MSM), 0.024% (10% diluted centrate), 0.028% (50% diluted centrate), and 0.177% (raw centrate (100% centrate)) on day 10. From these results, 100% centrate can be utilized for *Neochloris* sp. cultivation. Thus, photosynthetic biogas upgrading using *Neochloris* sp. can support the valorization of residual effluents such as digestate and biogas in the form of high added value pigments and biomass.

Keywords: Astaxanthin yield, decarbonization efficiency, *Neochloris* sp., photosynthetic biogas upgrading, wastewater treatment

**Acknowledgement**

I would like to express my deepest gratitude to my supervisor, Prof. Dr. Raul Muñoz Torre and Assistant Prof. Dr. Viktoriia Komarysta for all the guidance throughout my Master study. I sincerely appreciate his tremendous academic support, strict and warm encouragement, and for giving me many opportunities in his laboratory. I am also deeply thankful to my supervisor in Japan, Prof. Dr. Tatsuki Toda (Soka University) for giving me opportunities to study at Universidad de Valladolid for Master double degree program.

I appreciate all the professors in Escuela de Ingenierías Industriales at Universidad de Valladolid and members in the Institute of Sustainable Process for their encouragement and support to my laboratory life and life in Spain. I am deeply thankful to all administrative staff at Universidad de Valladolid and Soka University for their support to study in Spain.

## Index

# 1. Introduction (State of the art)

## 1.1. *Biogas as a renewable energy source*

Biogas is an attractive renewable energy source, unlike fossil fuels such as natural gas, oil and coal. This alternative energy resource is a byproduct of the anaerobic treatment of wastewater, organic fractions of municipal solid wastes (OMSW), livestock residues, or agroindustrial wastes. For example, anaerobic digestion is frequently used as an eco-friendly process for wastewater treatment or urban solid waste reduction. Anaerobic digestion converts the organic matter of wastewater into biogas containing methane ($CH_4$) and digestate containing residual organic carbon, nitrogen, and phosphorus. These byproducts can be used as energy sources and feedstocks for microalgal cultivation, respectively. The raw biogas is composed mainly of $CH_4$ (40-75%) and other gases such as $CO_2$ (15-60%), $H_2S$ (0.005-3%), nitrogen, and oxygen in a low proportion (less than 2%). In recent years, biogas has been considered a cornerstone to reduce greenhouse gas emissions and mitigate the environmental impact. Contamination by $CO_2$ from biogas causes environmental pollution and decreases the calorific value of biogas. $H_2S$ corrodes and damages boilers, gen-sets, as well as other equipment. Hence, these contaminating gases should be removed before the use of biogas.

## 1.2. *Biogas upgrading*

On a commercial scale, physical and chemical technologies are commonly used for biogas upgrading. For example, technologies such as in situ chemical precipitation, adsorption, absorption, and membrane separation are widely implemented. However, these technologies consume more energy and produce unwanted waste compared with biological methods. Contrary to physicochemical methods, biological methods such as biotrickling filtration, microaerophilic anaerobic digestion, and hydrogenotrophic $CO_2$ reduction to $CH_4$ do not require to use much solvent and expensive membranes and have been successfully tested in the previous research (Toledo-Cervantes et al., 2017a). However, these technologies entail high investment and operating costs because a pre-treatment and post-treatment (two-stage process) is required to remove the remaining $CO_2$ and $H_2S$ using physicochemical and biological methods. From this perspective, photosynthetic biogas upgrading is a promising biological alternative implemented in a single-stage process (Fig. 1). Compared to an activated carbon filter combined with a water scrubber (physicochemical methods), high-rate algal pond (HRAP) with a $CO_2$ absorption column (biological methods) showed lower operating costs and environmental impacts in terms of water consumption and greenhouse gas emission and achieved positive revenues after five years boosted by the sales of microalga biomass (Toledo-Cervantes et al., 2017a). However, the spread of this process is still limited by the economic viability due to the high photobioreactor surface areal requirement, the low cost of the products generated (biomethane and algal fertilizers), and the high investment cost (biomass drying unit for biomass dewatering for biofertilizer). In this context, synthesizing high-value-added products from microalgae grown on biogas is necessary for the economic sustainability of the process.

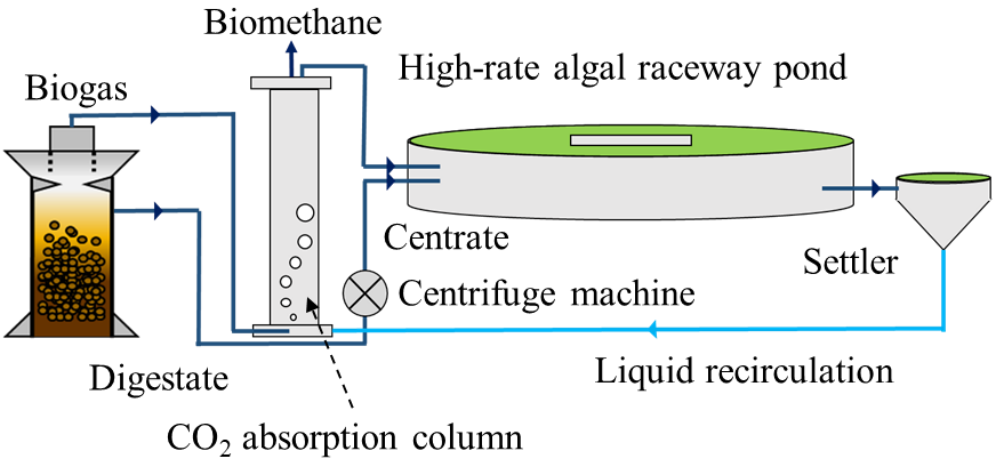


Fig. 1. Schematic diagram of the combined system of $CO_2$ absorption column and high-rate algal raceway pond for photosynthetic biogas upgrading.

### 1.3. *High market value of bioproducts and their applications*

Depending on the species, microalgae contain proteins, carbohydrates, lipids, and pigments. These compounds can be used as various bioproducts depending on the application. The use of whole microalgae is the simplest practical application, such as algal paste or dry flakes for foods, materials for combustion like biochar or biomass, and bio-oil. While, after pretreatments and extraction of microalgae, high-added-value bioproducts are available for practical application, including pigments such as chlorophyll, carotenoids, and phycobilin, lipids such as triacylglycerol and polyunsaturated fatty acids for biofuel and cosmetics, and proteins as a functional food. The choice of bioproduct with a specific microalgal species is essential to maximize the economic and environmental benefit of all over the process from cultivation to extraction.

Astaxanthin (3,3'-dihydroxy-β, β-carotene-4,4'-dione) is one of the most important bioproducts with several properties such as anti-inflammatory, anti-oxidative, anti-atherosclerotic, and anti-aging effects (Kishimoto et al., 2016; Farruggia et a., 2018; Eren et al., 2019). Thus, astaxanthin has been widely used in healthcare products for humans and as a feed for aquaculture and poultry industries (Zhang et al., 2014). Integration of wastewater treatment and production of astaxanthin with microalgae is cost-effective and eco-friendly but doubtful as a product for human consumption due to pathogen contamination and the fact that it is produced with wastewater. Therefore, astaxanthin from microalgae cultured with centrates is used for the aquaculture and poultry industries. In the aquacultural industry, astaxanthin or astaxanthin-rich microalgae has been used as a feed supplement for the growth of salmon, shrimp, and ornamental fish to enhance immunity (Ytrestøyl et al., 2006; Song et a., 2017). Unlike synthetic astaxanthin, feeding with natural astaxanthin could prevent antibiotics abuse and support a safe and natural pigmentation. In recent years, the demands for aquacultural feeds have been increasing because of the increase in aquaculture with the decrease in fisheries. Moreover, natural astaxanthin is attractive to enhance the immunity of animals for sustainable and eco-friendly aquaculture. For example, the mass shrimp culture is planned in Saudi Arabia as a government project for food security (Arab News, 2022). Thus, great space for natural astaxanthin is being created and developed. Natural astaxanthin price (1500 US$/ kg) is higher than that of artificial astaxanthin (1000 US$/ kg). From this high market value of bioproducts, other authors emphasized the importance of producing high-added-value products simultaneously with biogas upgrading to meet the economic feasibility in future studies

(Nagerajann et al., 2019). Nonetheless, there are few reports of research results aimed at coupling biogas upgrading, wastewater treatment and pigment production. In particular, the coupling photosynthetic biogas upgrading with the astaxanthin production has not been reported yet.

### 1.4. *Astaxanthin producer and production process*

*Haematococcus pluvialis* and *Chlorella zofingiensis* are widely used to produce natural astaxanthin on an industrial scale. Typically, esterified astaxanthin pigments exist in the resting cysts of algal cells (Ranjbar et al., 2008). The astaxanthin yield in *C. zofingiensis* is 0.06–0.5 % of the algal dry biomass (Zhang et al., 2016), while that in *H. pluvialis* is 5–6 % (Yang et al., 2016). Microalgae accumulate astaxanthin under stress conditions such as high light intensity, nutrient (nitrogen, phosphorus) deficiency, pH and salt stress, supplementation of excess acetate, and addition of hydrosulfide and organic acids to maintain the cellular redox imbalance (Yu et al., 2022; Nisar et al., 2015).

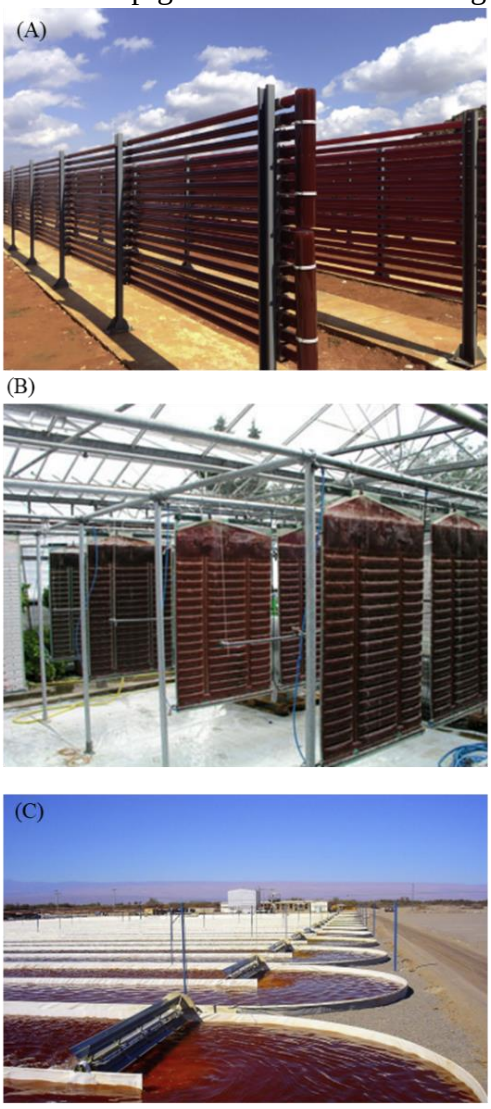

Fig. 2. Photograph of different cultivation systems for astaxanthin production; glass tubular photobioreactor by AstaBiotech(A), flat panel photobioreactor by Frauhofer IGB (B), and open raceway pond by Acatama-Bio (C).

Open raceway ponds or closed photobioreactors in batch, fed-batch, or continuous modes are available to culture *H. pluvialis* for industrial astaxanthin production, as shown in Fig. 2. As the culture conditions for maximum biomass productivity and astaxanthin accumulation differ, a two-step cultivation strategy is practical on a commercial scale. The first step is for the green phase to promote algal growth under appropriate culture conditions (optimum light intensity and sufficient nutrients availability). After the culture reaches high cell density, it enters the red inductive phase as a second step under the stress conditions (high light intensity, nutrients depletion). In the previous studies, astaxanthin productivities were 8 mg $L^{-1}$ $d^{-1}$ in 1.8-L tubular photobioreactor under outdoor conditions (García-Malea et al., 2009) and 4.3 mg $L^{-1}$ $d^{-1}$ in the open pond under indoor condition (Zhang et al., 2009). The closed photobioreactor reached higher astaxanthin productivity due to the low risk of contamination and ease of controlling the optimum culture condition despite high initial and operating costs compared to open ponds.

In the downstream of astaxanthin production, cell disruption and solvent extraction are necessary to separate astaxanthin from microalgae (Patel et al., 2022). Available processes for cell disruption include physical methods (bead beating, ultrasonication, high pressure), chemical methods (ionic liquid, organic solvent, acid treatment, nanomaterials), and biological methods (enzyme treatment, germination, milking). Acetone, ethyl acetate, ethanol, methanol, and dichloromethane are used as the solvents for extraction, and KOH for astaxanthin esters hydrolysis. From this perspective, technologies should be discussed in all processes, from upstream to downstream.

### 1.5. *Integration of photosynthetic biogas upgrading with astaxanthin production*

The choice of appropriate microalgal species is essential to achieve high $CO_2$ and $H_2S$ removal efficiency and high astaxanthin productivity. Even though optimizing process parameters in photosynthetic biogas upgrading is still under research, higher pH is one of the necessary conditions to improve $CO_2$ and $H_2S$ removal efficiency. At high pH, the carbonate/bicarbonate equilibrium triggers $CO_2$ capture in the bubble column (Bose et al., 2019). After uptaking bicarbonate by microalgae, the released hydroxide increases pH represented in Eq. (1). An increase in pH leads to carbonate regeneration and the formation of bicarbonate by $CO_2$ absorption (Eq. 2). Hydrogen sulfide is oxidized by bacteria using the high dissolved oxygen present in the recirculated cultivation broth, and sulfate precipitation occurs at high pH (9~11) without sulfur-oxidizing bacteria (Mieier et al., 2018; Posadas et al., 2015) as per the following Eq. (3). Thus, microalgae with tolerance to high pH are preferable as species for photosynthetic biogas upgrading. Additionally, microalgae with high $CO_2$ tolerance are desirable because the $CO_2$ concentrations in biogas vary from about 20% to 60%.

$$HCO_3^- \rightarrow CO_2 + OH^- \quad (1)$$

$$HCO_3^- + OH^- \rightarrow CO_3^{2-} + H_2O \quad (2)$$

$$2HS^- + 4O_2 \rightarrow 2H^+ + SO_4^{2-} \quad (3)$$

Although *H. pluvialis* typically contains the highest astaxanthin concentration among all microalgal strains, low biomass productivity and the long induction period of astaxanthin (8-12 days) limited its market scale (Wan et al., 2014). Moreover, *H. pluvialis* grows at the neutral pH in the growing phase and does not tolerate high $CO_2$ concentration. Chekanov et al. (2017) reported that $CO_2$-enriched air gas with 5% showed a beneficial effect on growth and astaxanthin accumulation, while 10% and 20% $CO_2$ were detrimental for growth. Thus, the supply of biogas containing high concentration of $CO_2$ (20-60%) could cause growth inhibition. Hence, this strain is not suitable for photosynthetic biogas upgrading. *Neochloris wimmeri* is known as a microalgal strain that can grow fast and accumulate astaxanthin (19.2 mg $g^{-1}$) at a similar yield as *H. pluvialis* (22.7 mg $g^{-1}$) (Orosa et al., 2001). At the Institute of Sustainable Processes, *Neochloris* sp. showed high growth at high pH (8~10) under a synthetic biogas atmosphere ($CH_4$: 70% and $CO_2$: 30%) in a preliminary experiment. Thus, *Neochloris* sp. is expected strain for coupling photosynthetic biogas upgrading with astaxanthin production simultaneously.

For high astaxanthin productivity, controlling the optimum culture condition is crucial to obtain a high growth rate and biomass yield. Additionally, low-cost cultivation is necessary to meet the economic feasibility. Domestic wastewater was applied as feedstock for microalgal cultivation to save the costs (Kang et al., 2006; Wu et al., 2013). However, microalgae can be inhibited by free ammonia ($NH_3$) converted from ammonium ions ($NH_4^+$) depending on the pH above 9.25 at 25°C (Eq.4). Free ammonia enters the cell by passive transport and interferes with the photosynthetic mechanism (Sekine et al., 2023). In terms of biogas composition, hydrogen sulfide can both enhance and inhibit microalgal growth. Klatt et al. (2015) reported that under low light intensity, $H_2S$ (0.15 mM) positively influences the rate of photosynthesis, which is determined by changes in the light-harvesting efficiency. However, $H_2S$ starts acting as an inhibitor above a certain threshold. The threshold of $H_2S$ concentration is species dependent. In this context, optimum conditions (pH control to prevent free ammonia inhibition, centrate dilution conditions, and $H_2S$ concentrations) are essential to maximize astaxanthin productivity.

$$NH_4^+ + OH^- \overset{pK=9.25}{\longleftrightarrow} NH_3 + H_2O \quad (4)$$

To our knowledge, there are few reports of research results aimed at coupling biogas upgrading and nutrient recovery from digestates with astaxanthin production. Especially the cultivation of *Neochloris* sp. for photosynthetic biogas upgrading using real centrate is reported for the first time. Therefore, the present study aimed at optimizing the cultivation of *Neochloris* sp. expected as an astaxanthin producer under different medium compositions and concentrations of $H_2S$ in biogas as a proof of concept.

## 2. Objectives

The aim of this study was to investigate the biogas decarbonization performance and biomass yield using *Neochloris* sp. as a model astaxanthin producer under the different dilution of centrate and different concentrations of $H_2S$ in biogas. The findings were compared with the biomass yield and astaxanthin yield with different species used in photosynthetic biogas upgrading and astaxanthin production to evaluate the potential of *Neochloris* sp. for coupling photosynthetic biogas upgrading with high-added-value bioproduct synthesis. Finally, the practical cultivation system for photosynthetic biogas upgrading and astaxanthin production is discussed.

## 3. Materials and Methods

### 3.1. *Microalgae and pre-culture conditions*

*Neochloris* sp. was discovered in the Novopokovka settlement, Chuguev district, Kharkiv region, Ukraine in 2015. The microalgae was precultured in 250 mL E-flasks with a mineral salt medium (MSM) composed of 6 g $L^{-1}$ $NaHCO_3$, 3 g $L^{-1}$ $Na_2CO_3$, 0.94 g $L^{-1}$ $K_2HPO_4$, 3.06 g $L^{-1}$ Na $NO_3$, 2.09 g $L^{-1}$ NaCl, 0.02 g $L^{-1}$ $CaCl_2$ $2H_2O$, 0.005 g $L^{-1}$ $FeSO_4$ $7H_2O$, and 0.1 g $L^{-1}$ $MgSO_4$ $7H_2O$ with 1 mL of micronutrients (Malik., 1983). The micronutrient solutions consisted of 3.1 g $L^{-1}$ $H_3BO_3$, 2.23 g $L^{-1}$ $MnSO_4$ $7H_2O$, 0.287 g $L^{-1}$ $ZnSO_4$ $7H_2O$, 0.088 g $L^{-1}$ $(NH_4)_6Mo_7O_{24}$ 4H2O, 0.146 g $L^{-1}$ $Co(NO_3)_2$ $4H_2O$, 0.033 g $L^{-1}$ $Na_2WO_4$ $H_2O$, 0.119 g $L^{-1}$ KBr, 0.083 g $L^{-1}$ KI, 0.154 g $L^{-1}$ $Cd(NO_3)_2$ $4H_2O$, 0.198 g $L^{-1}$ $NiSO_4(NH_4)_2SO_4$ $6H_2O$, 0.02 g $L^{-1}$ $VSO_4$ $2H_2O$, 0.474 g $L^{-1}$ $Al_2SO_4$ $KSO_4$ $24H_2O$, 0.037 g $L^{-1}$ $Cr(NO_3)_2$ $7H_2O$. The culture medium was maintained at 25ºC under continuous magnetic agitation at 200 rpm. Light intensity and the photoperiod were 300 µmol $m^{-2}$ $s^{-1}$ and 24 hours, respectively.

### 3.2. *Batch cultivation*

In this study, five experiments in batch mode to optimize *Neochloris* sp. cultivation conditions were tested. Figure 3 and Table 1 show the experimental planning, cultivation vessels used in this study, and media composition for each experiment, respectively. Firstly, the influence of different light intensities and dilution ratios of centrate from an anaerobic digestion system were examined when the bottle headspace was filled with air. Then, different strategies to avoid growth inhibition by free ammonia were tested. Subsequently, the influence of different biogas compositions on the removal efficiency of $CO_2$ and $H_2S$ was evaluated. Finally, the effect of different dilution of centrate on growth was investigated when the bottle headspace was filled with air. The batch experiments were carried out in 2.1-L glass bottles. Microalgae inoculum of 20 mL was inoculated into the bottles containing 180 mL of liquid media in all experiments. The photoperiod was maintained at 24 hours of continuous illumination. Cultivations were conducted until the steady state.

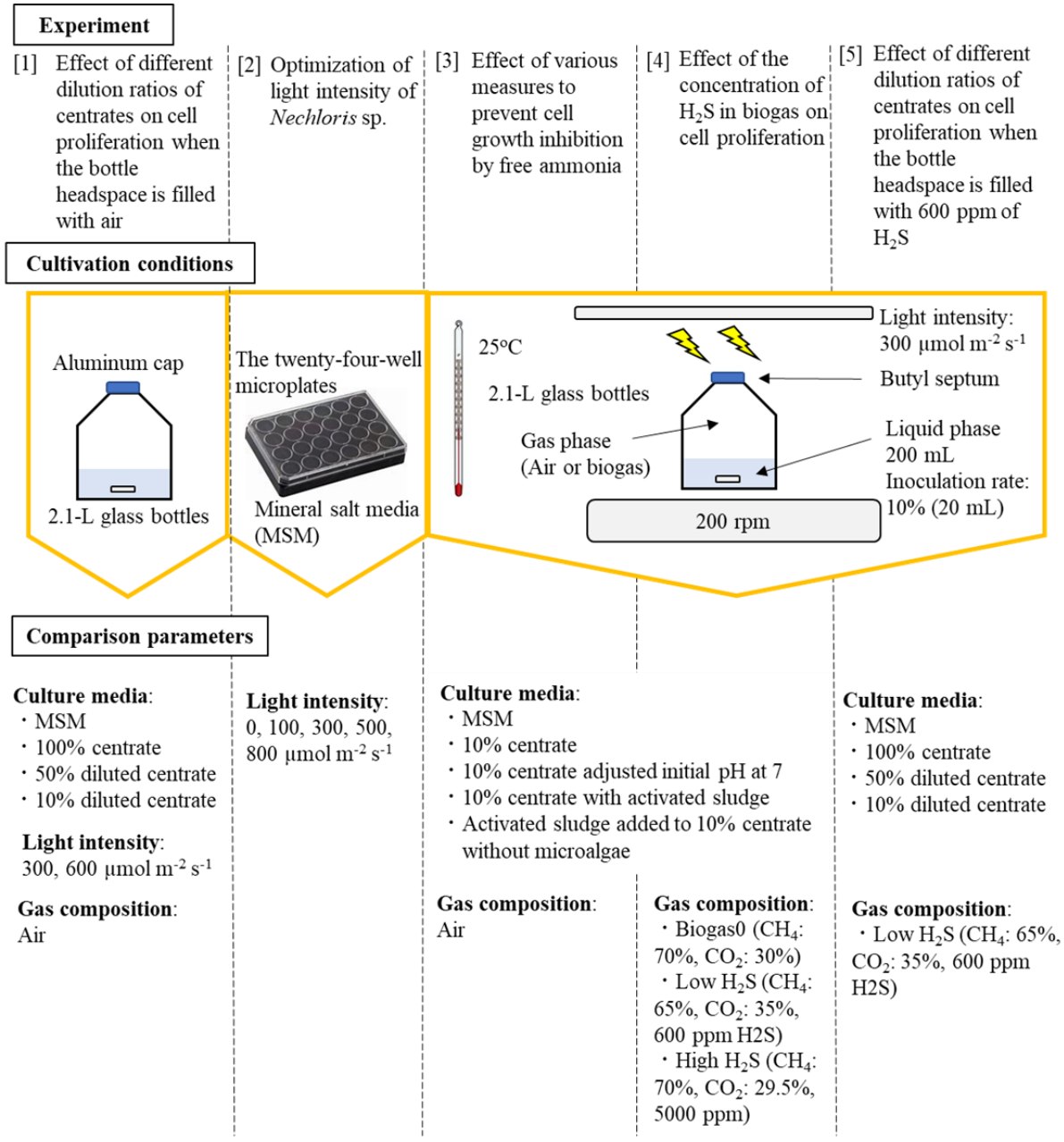


Fig. 3. Schematic experimental flows and culture vessels used in this study

Table 1. The composition of culture medium and purpose of each measure

| Experiments | Culture media | N-source | $NaHCO_3$/ $Na_2CO_3$ (g $L^{-1}$) | $FeSO_4$ $7H_2O$ (g $L^{-1}$) | $CaCl_2$ $2H_2O$ (g $L^{-1}$) | $MgSO_4$ $7H_2O$ (g $L^{-1}$) | Micronutrient (mL) | Purpose |
|---|---|---|---|---|---|---|---|---|
| All | MSM | Nitrate | 6/ 3 $NaHCO_3$ (g $L^{-1}$) | 0.005 | 0.02 | 0.1 | 1 | - |
| [1] | Centrate (100%, 50%, 10% dilution) | Ammonia | 4.2 | - | - | - | - | - |
| | 10% diluted centrate initial pH of 7 | Ammonia | 4.2 | 0.005 | 0.02 | 0.1 | 1 | HCl adjusted initial pH at 7 to prevent growth inhibition by free ammonia |
| [3], [4] | 10% diluted centrate with 2.5 mL activated sludge aliquot | Ammonia | 4.2 | 0.005 | 0.02 | 0.1 | 1 | Nitrifying bacteria in activated sludge perform nitrification, sulfur-oxidizing bacteria perform desulfurization. |
| | Activated sludge added to 10% diluted centrate without microalgae | Ammonia | 4.2 | 0.005 | 0.02 | 0.1 | 1 | To observe the growth kinetic of bacteria and potential contamination with other microalgal species |
| [5] | Centrate (100%, 50%, 10% dilution) | Ammonia | 4.2 | 0.005 | 0.02 | 0.1 | 1 | - |

### **3.3.** *Effect of different dilution ratios of centrates on cell proliferation when the bottle headspace was filled with air*

A centrate collected from Valladolid Wastewater Treatment Plant was centrifuged at 11000 rpm for 10 minutes and filtered twice by paper filters before and after autoclaving (121ºC, 20 min). Centrate without dilution (100%) and diluted 50% and 10% with distilled water were supplied into the bottles. The microalgal growth was compared for each centrate dilution and MSM as a control without biogas condition. Light intensities of 300 µmol $m^{-2}$ $s^{-1}$ and 600 µmol $m^{-2}$ $s^{-1}$ were examined.

### **3.4.** *Optimization of light intensity*

*Neochloris* sp. was cultured with MSM at different light intensities of 0, 100, 300, 500, and 800 µmol $m^{-2}$ $s^{-1}$. The twenty-four-well microplates were used as the cultivation containers with a 2-mL of effective volume. The temperature and light period were maintained 25ºC and 24 hours, respectively. During the experimental period, the optical density at 600 nm and 750 nm was measured after mixing the culture by pipetting every 24 hours.

### **3.5.** *Effects of various strategies to prevent cell growth inhibition by free ammonia*

Table 1 shows the comparative series and the purpose of each strategy. The centrate from Valladolid wastewater treatment plant is an $NH_4^+$-based feedstock, whose $NH_4^+$ can be converted to free ammonia at high pH (pK=9.25 at 25ºC), thus inhibiting microalgal growth. Therefore, adjustment of pH is important to prevent converting ammonium ions ($NH_4^+$) into free ammonia ($NH_3$). Controlling pH was performed by adding HCl on the initial day to set the pH of 7. As another strategy, a 2.5 mL activated sludge aliquot obtained from a lab-scale wastewater treatment plant was added to 200 mL centrate for nitrification. Activated sludge aliquot added to the assay without microalgae was prepared to observe the growth kinetic of bacteria and potential contamination with other microalgal species. In short, 10% diluted centrate, adjusted at initial pH of 7 with HCl (10% diluted centrate pH7) and 10% diluted centrate with activated sludge aliquot were compared with MSM and activated sludge aliquot added to 10% diluted centrate without microalgae as a control. As shown in Table 1, $NaHCO_3$

of 4.2 g $L^{-1}$, $CaCl_2$ $2H_2O$ of 0.02 g $L^{-1}$, $FeSO_4$ $7H_2O$ of 0.005 g $L^{-1}$, and $MgSO_4$ $7H_2O$ of 0.1 g $L^{-1}$, and 1 mL of micronutrients were added to compensate the nutrients present in MSM but absent in the centrate. Light intensities of 300 µmol $m^{-2}$ $s^{-1}$ were maintained under an illumination regime of 24 hours. After microalgae cultivation reached a steady state, light intensity converted from 300 µmol $m^{-2}$ $s^{-1}$ to 600 µmol $m^{-2}$ $s^{-1}$ during the astaxanthin induction phase (four days).

### 3.6. *Effect of the concentration of $H_2S$ in biogas on cell proliferation*

Bottles were initially filled with 180 mL of the medium, and the headspace of the bottles was flushed with helium for 10 min at a high flow rate to displace the air atmosphere. Bottles were closed with a butyl septum and an aluminum screw cap to avoid exchanging gas from the atmosphere. The headspace of the bottles was then flushed with synthetic biogas for 7 min and stabilized under continuous magnetic agitation at 200 rpm for more than one hour. The three different compositions of synthetic biogas were used: biogas 0: $CH_4$ (70%), $CO_2$ (30%); low $H_2S$ biogas: $CH_4$ (65%), $CO_2$ (35%), 600 ppm $H_2S$; high $H_2S$ biogas: $CH_4$ (70%), $CO_2$ (29.5%), 5000 ppm $H_2S$. Light intensities of 300 µmol $m^{-2}$ $s^{-1}$ were maintained under an illumination regime of 24 hours. After cells reached a steady state, the light intensity was changed to 600 µmol $m^{-2}$ $s^{-1}$ during the astaxanthin induction phase (four days).

### 3.7. *Effect of different dilution ratios of centrates on cell proliferation when the bottle headspace is filled with biogas containing 600 ppm of $H_2S$*

Centrate without dilution (100%), diluted 50% and 10% with distilled water were compared to MSM as a control for optimization of dilution ratios of centrate under the acidification of pH by $CO_2$ absorption. Light intensities of 300 µmol $m^{-2}$ $s^{-1}$ were set up in the growth phase. After cell reached stationary phase, the light intensity was changed to 600 µmol $m^{-2}$ $s^{-1}$ during the astaxanthin induction phase (four days).

### 3.8. *Sampling and analytical methods*

Aliquots of 4 mL of cultivation broth were drawn every day to monitor culture absorbance at 600 nm and 750 nm using a spectrophotometer (BMG LABTECH, Germany). The samples were centrifuged at 1330 rpm for 10 min and used as a blank to remove suspended maters in centrate for monitoring the correct turbidity of microalgal growth. The specific growth rate (µ: $d^{-1}$) of *Neochloris* sp. was calculated using equation (5).

$$\mu = \ln(X_2 - X_1)/\left((t_2 - t_1)\right) \quad (5)$$

where $X_1$ and $X_2$ are $OD_{750}$ at time $t_1$ and $t_2$ (d), respectively. The correlation between total suspended solids (TSS: g $L^{-1}$) and absorbance of *Neochloris* sp. at 600 and 750 nm was calculated using equation (6-1) and (6-2).

$$\mathrm{TSS} = 0.87308\ \mathrm{OD}_{600} \quad (6\text{-}1)$$

$$\mathrm{TSS} = 0.88439\ \mathrm{OD}_{750} \quad (6\text{-}2)$$

where $OD_{600}$ and $OD_{750}$ were the absorbances of *Neochloris* sp. Biomass productivity of microalgae (g $L^{-1}$ $d^{-1}$) was calculated using equation (7).

$$P = \frac{TSS_t - TSS_0}{t} \quad (7)$$

where $TSS_t$ and $TSS_0$ is total suspended solids concentration on day t and 0 (g $L^{-1}$) and t is the culturing time (d). The pH, inorganic carbon, and total nitrogen were also measured using a pH meter and TOC-Analyzer (Shimadzu, Japan), respectively. The concentration of $NO_3^-$, $NO_2^-$, $SO_4^{2-}$, and $PO4_3^-$ were analyzed by HPLC-IC, and a 100 µL headspace sample was used for gas concentration measurements ($CH_4$, $CO_2$, $H_2S$, $O_2$) using a gastight syringe (Hamilton,

USA) and a CP-3800 gas chromatograph equipped with a thermal conductivity detector (Agilent, USA). The light intensity was measured using an LI-250A (LI-COR, USA) before cultivation.

### *3.9. Astaxanthin content quantification*

For the pigment analysis, biomass was collected in the starting day of the astaxanthin induction phase (high light intensity) and the final day. Samples were centrifuged at 6000 rpm for 10 min and stored at −20°C until further use. Cell disruption and solvent extraction were conducted according to the analysis methods by Cyanotech (2013). Cells collected in the 50-mL conical tube were washed with deionized water until the neutral reaction of the discarded supernatant. The washed samples were placed into the screwed cap Eppendorf tubes with 100 mg of quartz powder. The samples adding DMSO solution were placed into the preheated air convection bath at 43-46°C for 5 min. After 5 min, the cells were ground in the bead beater for 5 min and repeated two times. After a second repetition, the samples were centrifuged at 13300 rpm for 10 min, and the supernatants were placed into a 25-mL volumetric flask. The pellets in the tube were supplemented with 1-mL acetone containing 500 mg $L^{-1}$ of butylated hydroxyanisole. The pellets were grounded for 5 min and centrifuged at 13300 rpm for 10 min and repeated for 4-5 times until the colorless pellet. The volumetric flask with the supernatant was measured up, and its absorbency was measured at 474 nm. Total carotenoids were calculated using equation (8-1) and (8-2).

$$\text{Total carotenoids (mg)} = OD_{474} \times V \times DR/\ 210 \quad (8\text{-}1)$$

$$\text{Astaxanthin (\%)} = \text{Total carotenoids (mg)} \times 85\%/\ TSS_{biomass}\ \text{(mg)} \quad (8\text{-}2)$$

where, V is acetone volume (mL), DR is the dilution ratio of the samples with acetone, and 210 is the extinction coefficient of astaxanthin in acetone. For the hydrolysis of the biomass, the samples adjusted pH of 7 by adding 2.5-mL of 0.05 M Tris buffer were added 100-µL of cholinesterase stock solution as an enzyme. The samples were incubated in the preheated water bath at 40°C for 45 min and mixed frequently. 0.5 g of anhydrous sodium sulfate and 2-mL of cyclohexane were added to the samples, mixed by vortex, and centrifuged for 5 min. The upper cyclohexane layer was transferred into the separate clean and dry screwed cap vials. The bottom samples were repeatedly washed with cyclohexane 3-4 times until cyclohexane became colorless. The samples were evaporated by inert gas flushing. After ensuring no water was present in the test tube, the samples were dissolved in 3 mL of methyl tert-butyl ether (MTBE) and transferred into HPLC vials. All procedures for the extraction were conducted under subdued light to prevent photodegradation of the pigments.

The standards and samples were injected into high-performance liquid chromatography (HPLC) using C30 bonded silica-based reversed-phase column (250 × 4.6 mm inner diameter, 5µm, YMC CO. LTD, Japan). The HPLC flow rate was 1.0 mL/ min: column temperature 25°C. The HPLC conditions were performed using 81: 15: 4 (v/ v/ v) methanol, MTBE, and water as an eluent A and 6: 90: 4 (v/ v/ v) methanol, MTBE, and water as an eluent B. The gradient elution was performed from initial conditions of 0% of eluent B at 0 min, followed by 100% of eluent B at 90 min. The standard curve and the retention times were calibrated using astaxanthin and $\beta$-carotene standards in MTBE. All results were expressed as milligram per gram TSS of microalgal biomass (mg $g^{-1}$). Astaxanthin productivity (mg $L^{-1}$ $d^{-1}$) was calculated by astaxanthin content multiplied by biomass productivity.

### **3.10.** *Statistical method*

A one-way ANOVA analysis of variance was conducted to determine the significance of the values obtained by performing a Tukey-Kramer test with a value of $p < 0.05$ considered significant.

## 4. Results and Discussions

### 4.1. *Effect of different ratios of centrate on cell proliferation when the bottle headspace is filled with air & optimization of light intensity*

The growth of *Neochloris* sp. was compared at different dilutions of centrates (100%, 50%, 10%) and MSM at a light intensity of 600 µmol $m^{-2}$ $s^{-1}$. The initial biomass concentration of MSM, 100%, 50%, and 10% diluted centrates were 0.11±0.0097 g $L^{-1}$, 0.13±0.0066 g $L^{-1}$, 0.15±0.032 g $L^{-1}$, and 0.10±0.016 g $L^{-1}$, respectively. The growth of *Nechloris* sp. was not observed for 8 days (Fig. 4A). pH for each condition did not show significant variations from the first day (MSM: 9.3, 100%: 8.41, 50%: 8.35, 10%: 8.45) to the final day (MSM: 9.67, 100%: 9.27, 50%: 9.15, 10%: 8.96). It was concluded that photoinhibition limited the growth of *Nechloris* sp.

Thus, the optimum light intensity for *Neochloris* sp. was investigated. From the result of optimization of the light intensity, the specific growth rate and TSS at 300 µmol $m^{-2}$ $s^{-1}$ showed the highest value compared to other light intensities (0, 100, 500, 800 µmol $m^{-2}$ $s^{-1}$) (Fig. 5A). The specific growth rate was calculated from day 2 to day 4 and accounted for 0.00070 $d^{-1}$ (0 µmol $m^{-2}$ $s^{-1}$), 0.30 $d^{-1}$ (100 µmol $m^{-2}$ $s^{-1}$), 0.35 $d^{-1}$ (300 µmol $m^{-2}$ $s^{-1}$), 0.0033 $d^{-1}$ (500 µmol $m^{-2}$ $s^{-1}$), and −0.13 $d^{-1}$ (800 µmol $m^{-2}$ $s^{-1}$), respectively (Fig. 5B). The significant difference was determined between 100 µmol $m^{-2}$ $s^{-1}$ and 0, 500, 800 µmol $m^{-2}$ $s^{-1}$. The specific growth rate at a light intensity of 300 µmol $m^{-2}$ $s^{-1}$ was also significantly higher than that at 0, 500, and 800 µmol $m^{-2}$ $s^{-1}$. TSS at 300 µmol $m^{-2}$ $s^{-1}$ was significantly higher than that of other light intensities (Fig. 5C). From these results, the optimum light intensity of *Neochloris* sp. was concluded to be 300 µmol $m^{-2}$ $s^{-1}$.

Considering the result of optimization of light intensity, the subsequent experiment was conducted at 300 µmol $m^{-2}$ $s^{-1}$ with different dilution ratios of centrate (100%, 50%, 10% dilution). Only microalgae grown in MSM showed increase of optical density at 750 nm and pH, and showed maximum TSS of 0.75±0.026 g $L^{-1}$ (day 9) and pH of 10.44, respectively (Fig. 4B, C). The assay conducted with centrate did not show an increase in the microalgal growth due to possibly ammonia inhibition and lack of certain nutrients such as $Fe^{2+}$, $Ca^{2+}$, and $Mg^{2+}$. The utilization of ammonia and its threshold of inhibition depends on the species. $EC_{50}$ is shown as a 50% inhibitory concentration of $NH_3$. Its value for *Arthrospira platensis* (NIES-39), *Arthrospira fussiformis* (UTEX-2721), *Synechococcus leopoliensis* (NIES-3277), and *Anabaena cylindrica* (NIES-19) are reported at 84.6 mg-$NH_3$ $L^{-1}$, 85.9 mg-$NH_3$ $L^{-1}$, 74.5 mg-$NH_3$ $L^{-1}$, and 12.6 mg-$NH_3$ $L^{-1}$, respectively (Sekine et al., 2023). Under alkalinity culture conditions (pK>9.25, 25°C), ammonium ions convert to free ammonia. Thus, pH control is essential for using centrate as a feedstock for microalgal cultivation.

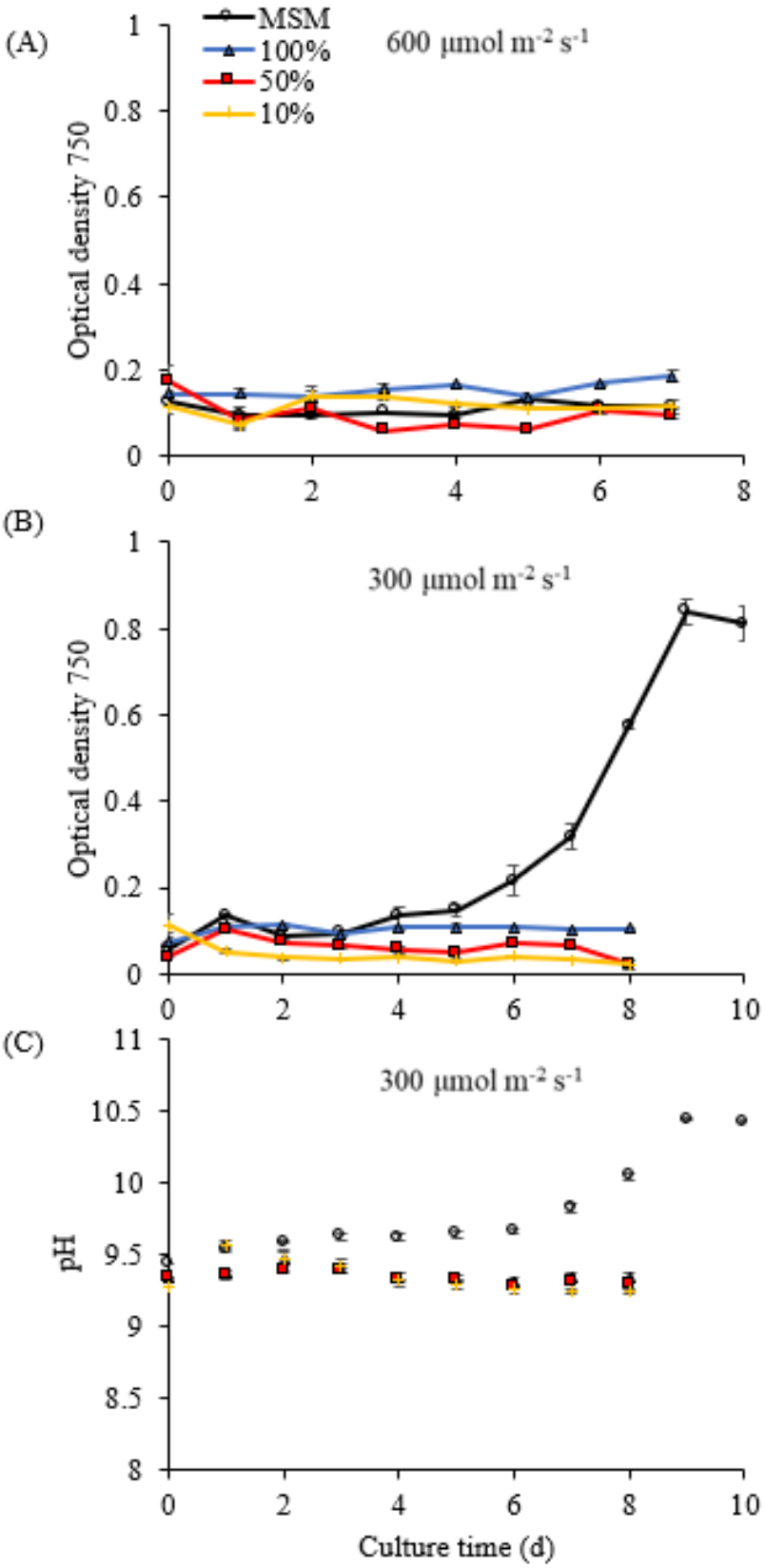


Fig. 4. Time course of the optical density at 750 nm with PAR of 600 µmol $m^{-2}$ $s^{-1}$ (A), OD 750 nm (B) and pH (C) with PAR of 300 µmol $m^{-2}$ $s^{-1}$ under MSM and different concentrations of centrate.

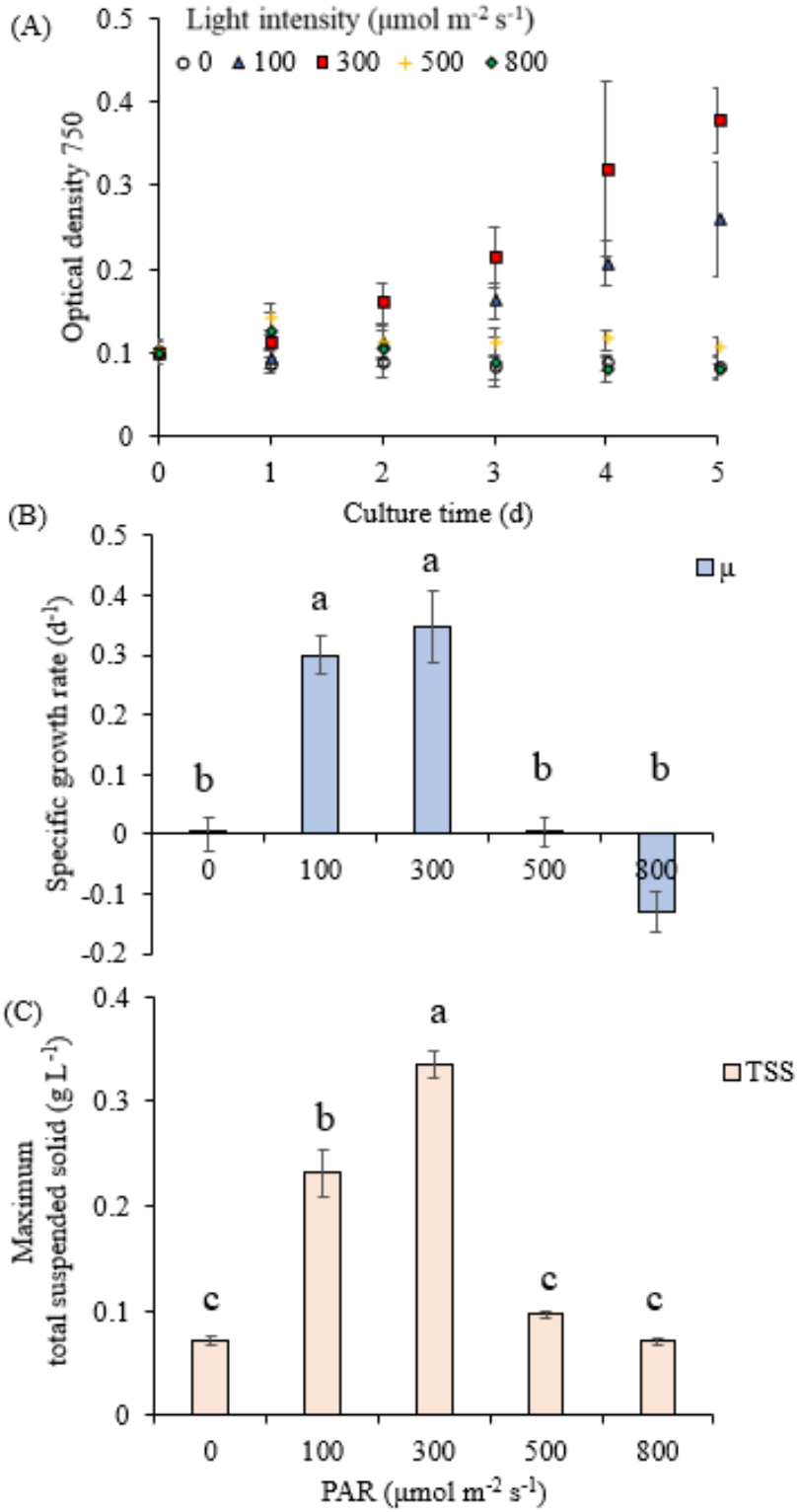


Fig. 5. Time course of the optical density at 750 nm (A), specific growth rate (B), and the maximum TSS (C) under different PAR. One-way ANOVA of variance followed by Tukey-Kramer test was used to determine the significance of the value ($p$<0.05).

### 4.2. *Effect of various strategies to prevent cell growth inhibition by free ammonia*

From the results in previous experiments, this experiment supplemented culture broth with nutrients such as $Fe^{2+}$, $Ca^{2+}$, and $Mg^{2+}$ into the centrate and tried some strategies to prevent growth inhibition by free ammonia as shown in Table 1. Different media were tested for the strategies to prevent free ammonia inhibition, each with a pH control and nitrification, with the addition of HCl and activated sludge aliquot, respectively. Under the condition where the air is injected into the headspace of bottles, the optical density of MSM increased from day 1 and reached a steady state on day 5 (Fig. 6A). The maximum TSS of MSM were 0.79±0.0071 g $L^{-1}$ on day 6. Although the 10% diluted centrate did not support an increase in TSS, the 10% diluted centrate adjusted initial pH of 7 supported a slight increase on day 7. The changes in pH also showed a similar trend with optical density (Fig. 6B). However, optical density in 10% diluted centrate adjusted initial pH of 7 did not increase after day 7 due to ammonia inhibition. In this study, sodium nitrate was used in MSM, while the nitrogen source in the domestic wastewater was mostly ammonium ions. High pH inhibited the growth of these microalgae caused by the share of ammonium ions converted to free ammonia over pH of 9.25 at 25°C (Giorgos et al., 2014). To increase microalgal growth using an ammonia-based medium like centrate from wastewater, another pH control is an essential operation. The optical density in the assays conducted with centrate diluted at 10% with activated sludge aliquot and the assay conducted with activated sludge aliquot added to 10% diluted centrate without microalgae increased from day 5 (Fig. 6A). From microscopic observation, the assay conducted with 10% diluted centrate with activated sludge aliquot was contaminated with other microalgae, which were tentatively determined as *Chlorella* sp. from its size and was dominant against *Neochloris* sp. In this case, *Neochloris* sp. coexisted with *Chlorella* sp. and grew as well as with MSM.

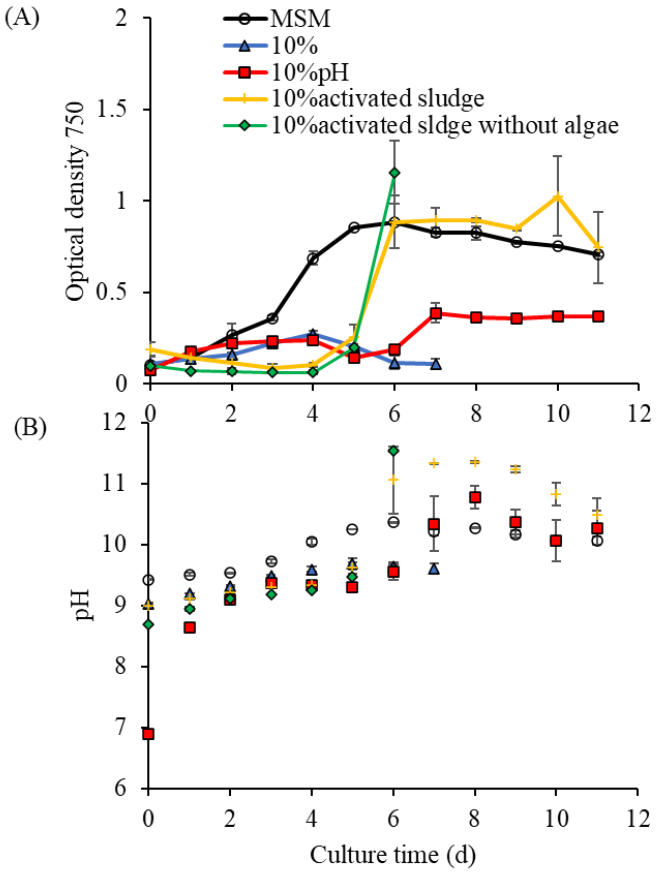


Fig. 6. Time course of the optical density at 750 nm (A) and pH (B) under different medium conditions.

### 4.3. *Effect of the concentration of $H_2S$ in biogas on cell proliferation*

Biogas0 ($CH_4$: 70%, $CO_2$: 30%) injected into the headspace of the bottles significantly increased optical density compared with the assays supplemented just with air. Optical density of centrate diluted at 10%, 10% diluted centrate adjusted initial pH of 7, and 10% diluted centrate with activated sludge aliquot showed a similar trend and reached a steady state on day 5 (Fig. 7A). Maximum TSS were obtained at 2.57±0.92 g $L^{-1}$ (MSM), 3.74±0.064 g $L^{-1}$ (10% diluted centrate), 3.50±0.38 g $L^{-1}$ (10% pH7), and 3.55±0.38 g $L^{-1}$ (10% with activated sludge aliquot), respectively, and there was no significant difference for each condition. In this case, pH values were maintained below 9.25 until day 5 under the condition of 10% diluted centrate and 10% diluted centrate adjusted initial pH of 7 and 10% diluted centrate with activated sludge aliquot due to the dissolution of $CO_2$ by injecting biogas into the headspace of the bottles (Fig. 7B). For the time course of the gas composition of the headspace in the bottles, $CO_2$ under the condition of 10% diluted centrate, 10% diluted centrate adjusted initial pH of 7, and 10% diluted centrate with activated sludge aliquot was removed faster than under MSM. These conditions obtained $CO_2$ removal efficiency of 97.4% (MSM) on day 7, 95.9% (10% diluted centrate) on day 5, 95.7% (10% pH 7) on day 5, and 97.6% (10% diluted centrate with activated sludge aliquot) on day 5 (Table 2). Compared with the use of nitrate form as a nitrogen-source in the culture medium, microalgae preferentially consumed ammonium nitrogen because its assimilation uses less energy than other a nitrogen-sources (Florencio and Vega, 1983; Perez-Garcia et al., 2011). Wang and Lan (2011) reported that *Neochloris oleoabundans* consumed ammonia faster than nitrate as a nitrogen source. Thus, this study indicated that the combination of acidification by the $CO_2$ present in biogas and $NH_4^+$-based centrate slightly promoted assimilation of $CO_2$ by *Neochloris* sp.

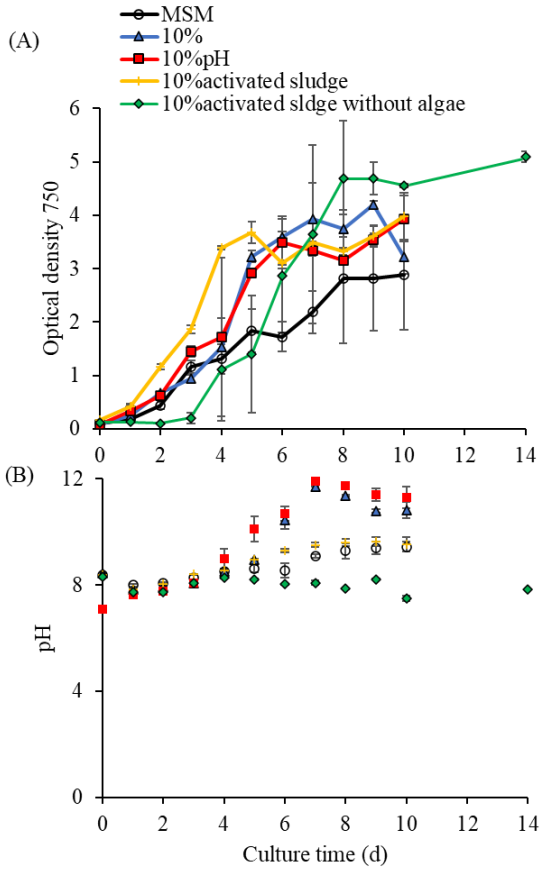


Fig. 7. Time course of the optical density at 750 nm (A) and pH (B) under different medium conditions with biogas0 ($CH_4$: 70%, $CO_2$: 30%) in the headspace of the bottles.

Table 2 $CO_2$ removal efficiency in this study

| | Medium conditions | day | 0 ppm | day | 600 ppm | day | 5000 ppm |
|---|---|---|---|---|---|---|---|
| $CO_2$ removal efficiency (%) | MSM | 7 | 97.4 | 14 | 87.1 | 9 | 3.3 |
| | 10% centrate | 5 | 95.9 | 9 | 99.0 | 9 | 1.2 |
| | 10% centrate adjusted initial pH at 7 | 5 | 95.7 | 8 | 99.8 | 9 | 3.3 |
| | 10% centrate with activated sludge | 5 | 97.6 | 14 | 82.8 | 8 | 97.3 |

Biogas with 600 ppm $H_2S$ stimulated microalgal growth in this study (Fig. 8). Compared to TSS under the headspace of biogas without $H_2S$, biogas containing 600 ppm $H_2S$ increased almost two-fold TSS in all medium conditions (Fig. 12). Maximum TSS with 10% diluted centrate and 10% diluted centrate adjusted initial pH of 7 were obtained at 6.98±0.029 g $L^{-1}$ and 6.41±0.47 g $L^{-1}$ on day 9, respectively. This result demonstrated that supplements of low 600 ppm $H_2S$ enhanced the growth of *Neochloris* sp. and the mixed culture of microalgae and bacteria. Moreover, decarbonization in biogas was also achieved. The $CO_2$ removal efficiency was 87.0% (MSM) on day 14, 98.9% (10% diluted centrate) on day 9, 99.8% (10% pH7) on day 8, 82.8% (10% diluted centrate with activated sludge aliquot) on day 14, respectively. Thus, it can be concluded that *Neochloris* sp. grew and removed $CO_2$ effectively under the headspace of 600 ppm $H_2S$. Klatt et al. (2015) reported that $H_2S$ concentration below 0.15 mM positively increased the efficiency and recovery rate of photosynthesis using cyanobacteria under low light intensity. Besides, Cheng et al. (2019) showed that the biomass yield and maximum quantum yield of PSII photochemistry (*Fv/Fm*) of *Nannocloropsis Oceania* increased by 28.2% and 65.5%, respectively, with 0.5 NaHS as the $H_2S$ donor. This is because low concentrations of $H_2S$ below the threshold improve DNA and RNA synthesis, translation initiates by eIF-2 with ribosomal proteins and increases the contents of both photosynthetic pigments (Chl *a*), and light harvesting proteins. Similar to the previous study, this study indicated that 600 ppm $H_2S$ enhanced the growth of *Neochloris* sp. For the time course of nutrients under the headspace of biogas without $H_2S$ and with 600 ppm $H_2S$, inorganic carbons slightly decreased in 10% diluted centrate. IC in MSM was maintained until the end of cultivation because the carbonate/bicarbonate equilibrium triggers $CO_2$ capture in the culture media (Fig. 9A, C). Therefore, pH in MSM was relatively maintained. Total nitrogen decreased in all medium compositions and were depleted under the centrate conditions but remained in MSM (Fig. 9B, D). From microscopic observation, *Neochloris* sp. made symbiotic consortia with bacteria and *Chlorella* sp. under the headspace of 10% centration with activated sludge aliquot (Fig. 13B, E). When 0 ppm and 600 ppm $H_2S$ of biogas, *Chlorella* sp. was dominant against *Neochloris* sp., and these microalgae grew as well as other medium conditions.

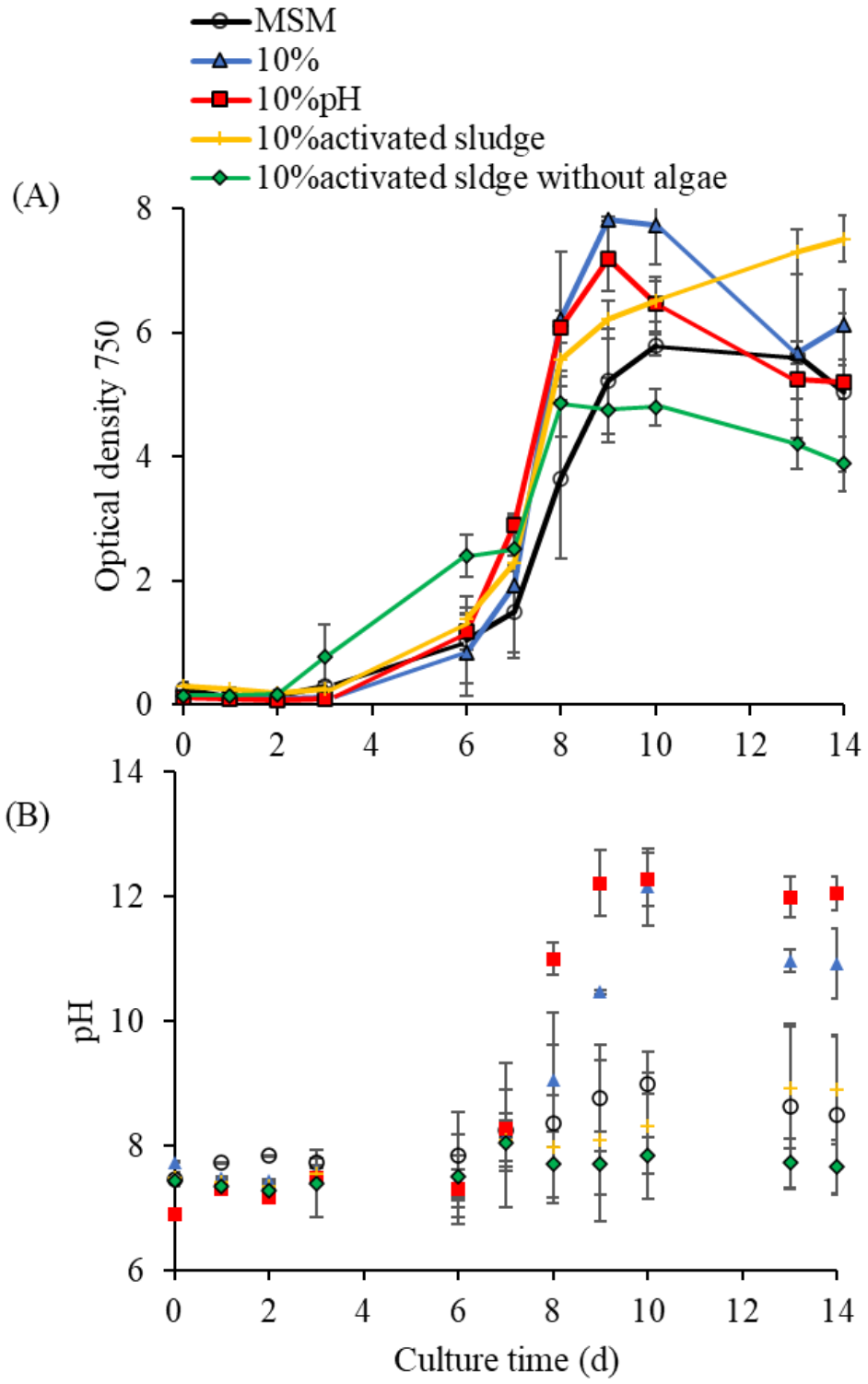


Fig. 8. Time course of the optical density at 750 nm (A) and pH (B) under different medium conditions with biogas contained low $H_2S$ ($CH_4$: 65%, $CO_2$: 35%, $H_2S$: 600 ppm) in the headspace of the bottles.

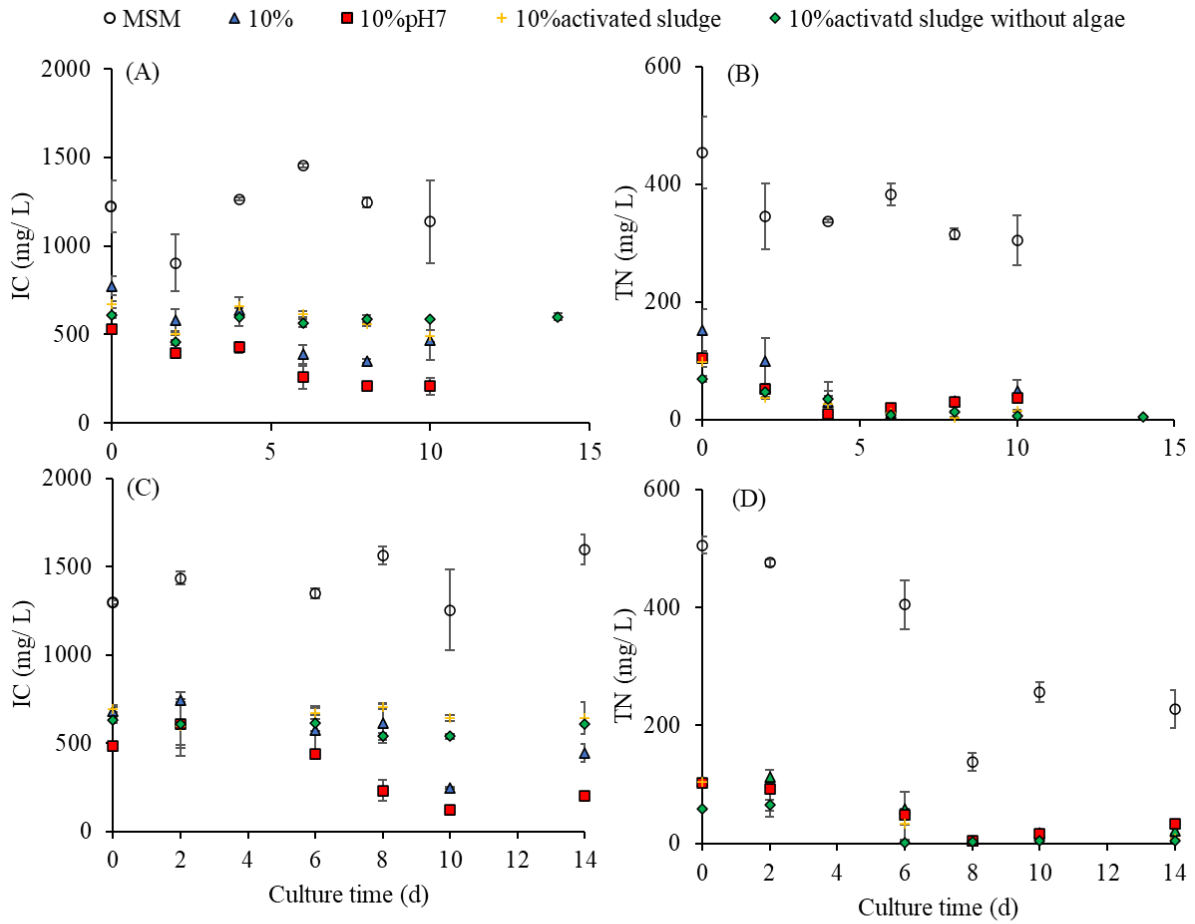


Fig. 9. Time course of total inorganic carbon (A) and total nitrogen (B) under different medium conditions with biogas0 ($CH_4$: 70%, $CO_2$: 30%) in the headspace of the bottles. Time course of total inorganic carbon (C) and total nitrogen (D) under different medium conditions with biogas including 600 ppm $H_2S$($CH_4$: 65%, $CO_2$: 35%, $H_2S$: 600 ppm) in the headspace of the bottles.

Contrary to biogas without $H_2S$ and with 600 ppm $H_2S$, biogas with 5000 ppm inhibited the growth of *Neochloris* sp. except for the condition of 10% diluted centrate with activated sludge aliquot (Fig. 10A). $H_2S$ is known as a potent inhibitor of oxygenic photosynthesis (Ohki et al., 2012). The threshold of the concentration of $H_2S$ is species dependent (Lisjak et al., 2013). The removal efficiency of $CO_2$ was obtained at 97.3% on day 8. With 5000 ppm $H_2S$, TSS of 10% diluted centrate with activated sludge aliquot was at 4.36±0.057 g $L^{-1}$ but lower than that with 600 ppm $H_2S$ (Fig. 12). From microscopic observation, the condition of 10% diluted centrate with activated sludge aliquot showed the growth of microalgae. Especially, even though *Chlorella* sp. was dominant against *Neochloris* sp. with biogas containing bellow 600 ppm $H_2S$, *Neochloris* sp. was dominant against other bacteria and *Chlorella* sp. with biogas containing 5000 ppm $H_2S$ (Fig. 13F). *Neochloris* sp. probably acclimatize to $H_2S$, and sulfur-oxidizing bacteria performed desulfurization. The gradual phenomenon of adaptation to $H_2S$ was reported (Cheng et al., 2019). In hypothesis, sulfur-oxidizing bacteria help to decrease the concentration of $H_2S$ below the threshold and *Neochloris* sp. acclimatized to $H_2S$ during the lag phase (Fig. 10A). As a result, with 5000 ppm, *Neochloris* sp. grew faster than *Chlorella* sp. The adjustment of concentration of $H_2S$ can be crucial parameter to control the dominant species in mixed

cuture. Thus, further study is necessary to confirm the acclimatizing speed depending on species and concentration of $H_2S$. Moreover, the evaluation of the dominant ratio of different microalgal species and astaxanthin production is important to see the effectiveness of the addition of activated sludge aliquot on astaxanthin production. As shown Fig. 11, inorganic carbon decreased after day 4 in 10% diluted centrate with activated sludge aliquot and activated sludge aliquot added to 10% diluted centrate without microalgae with the increase of optical density at 750. As same as inorganic carbon, symbiosis of *Neochloris* sp. and *Chlorella* sp. in the assay conducted with 10% diluted centrate with activated sludge aliquot suddenly consume nitrogen resources after day 4.

In summary of the effect of different concentration of $H_2S$ in biogas, *Neochloris* sp. with biogas containing 600 ppm $H_2S$ obtained significantly higher biomass yield of 6.98±0.029 g $L^{-1}$ than other gas composition (Fig. 12). Moreover, addition of activated sludge aliquot was effective to treat biogas with high concentration of $H_2S$ (5000 ppm).

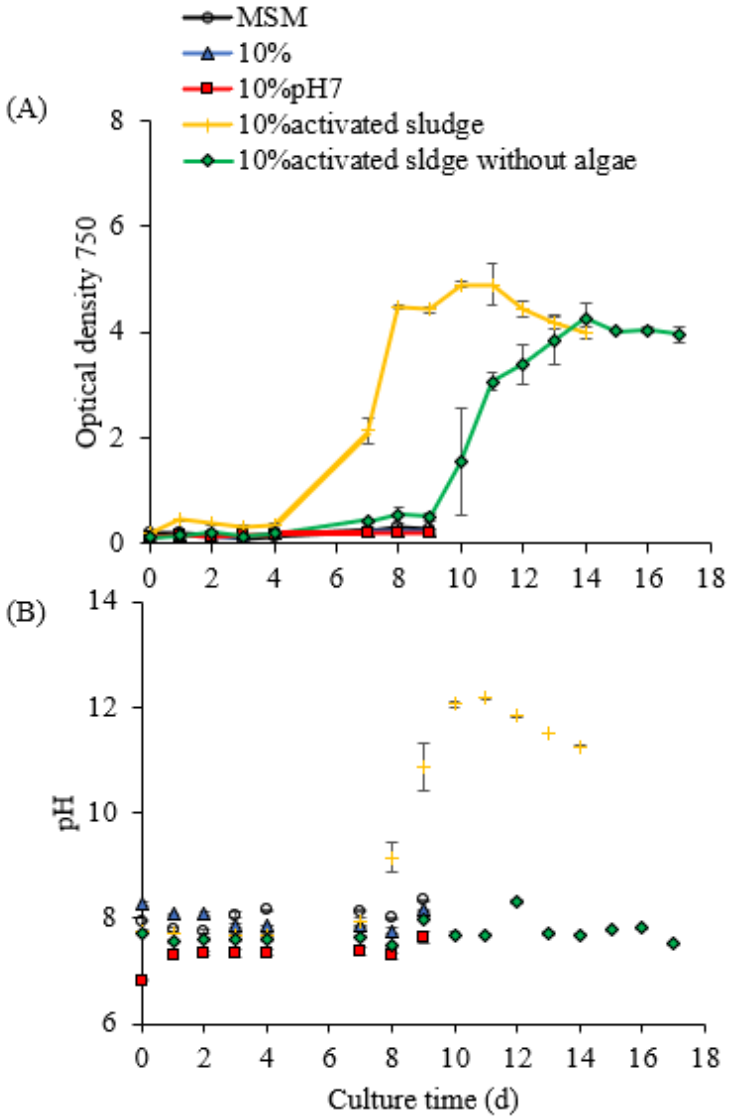


Fig. 10. Time course of the optical density at 750 nm (A) and pH (B), under different medium conditions with biogas contained high $H_2S$ ($CH_4$: 70%, $CO_2$: 29.5%, $H_2S$: 5000 ppm) in the headspace of the bottles.

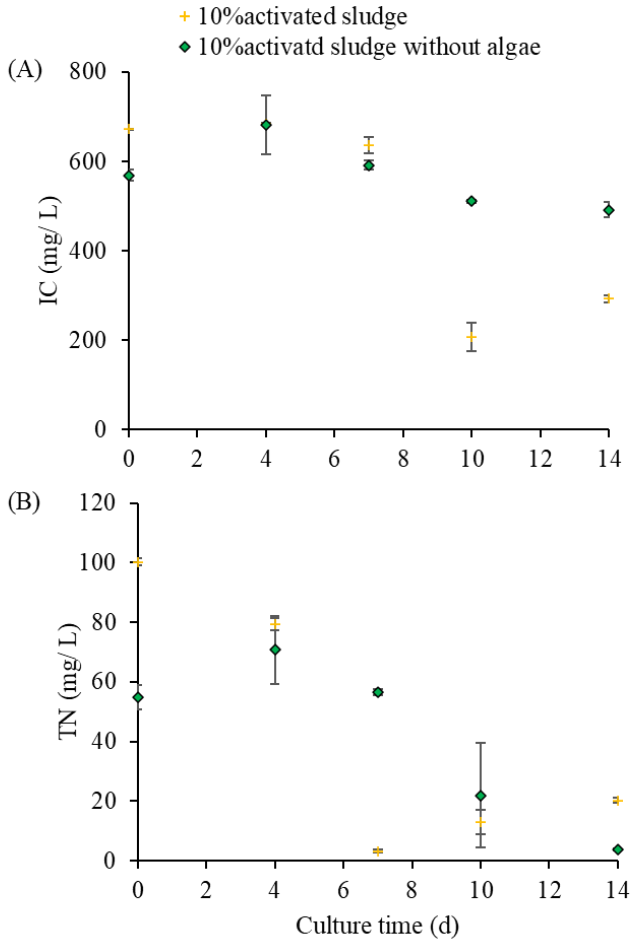


Fig. 11. Time course of total inorganic carbon (A) and total nitrogen (B) under different medium conditions with biogas contained high $H_2S$ ($CH_4$: 70%, $CO_2$: 29.5%, $H_2S$: 5000 ppm) in the headspace of the bottles

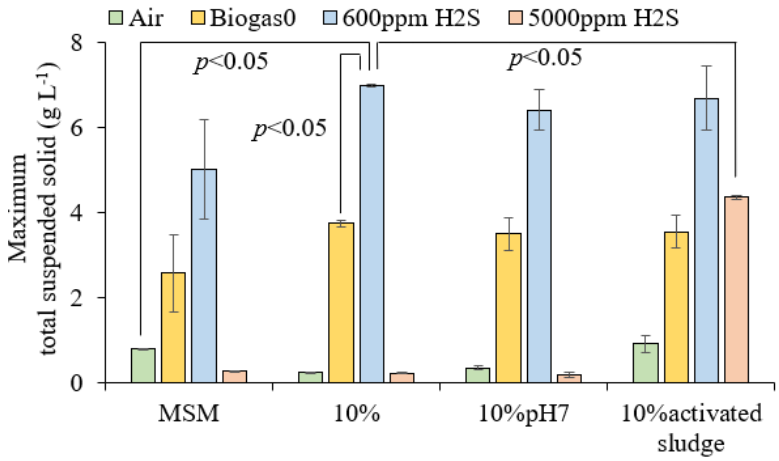


Fig. 12. Maximum total suspended solid of biomass with different gas composition of headspace in the bottles (Air, Biogas0 [$CH_4$: 70%, $CO_2$: 30%], Low $H_2S$ [$CH_4$: 65%, $CO_2$: 35%, $H_2S$: 600 ppm], High $H_2S$ [$CH_4$: 70%, $CO_2$: 29.5%]). One-way ANOVA of variance followed by Tukey-Kramer test was used to determine the significance of the value ($p$<0.05).

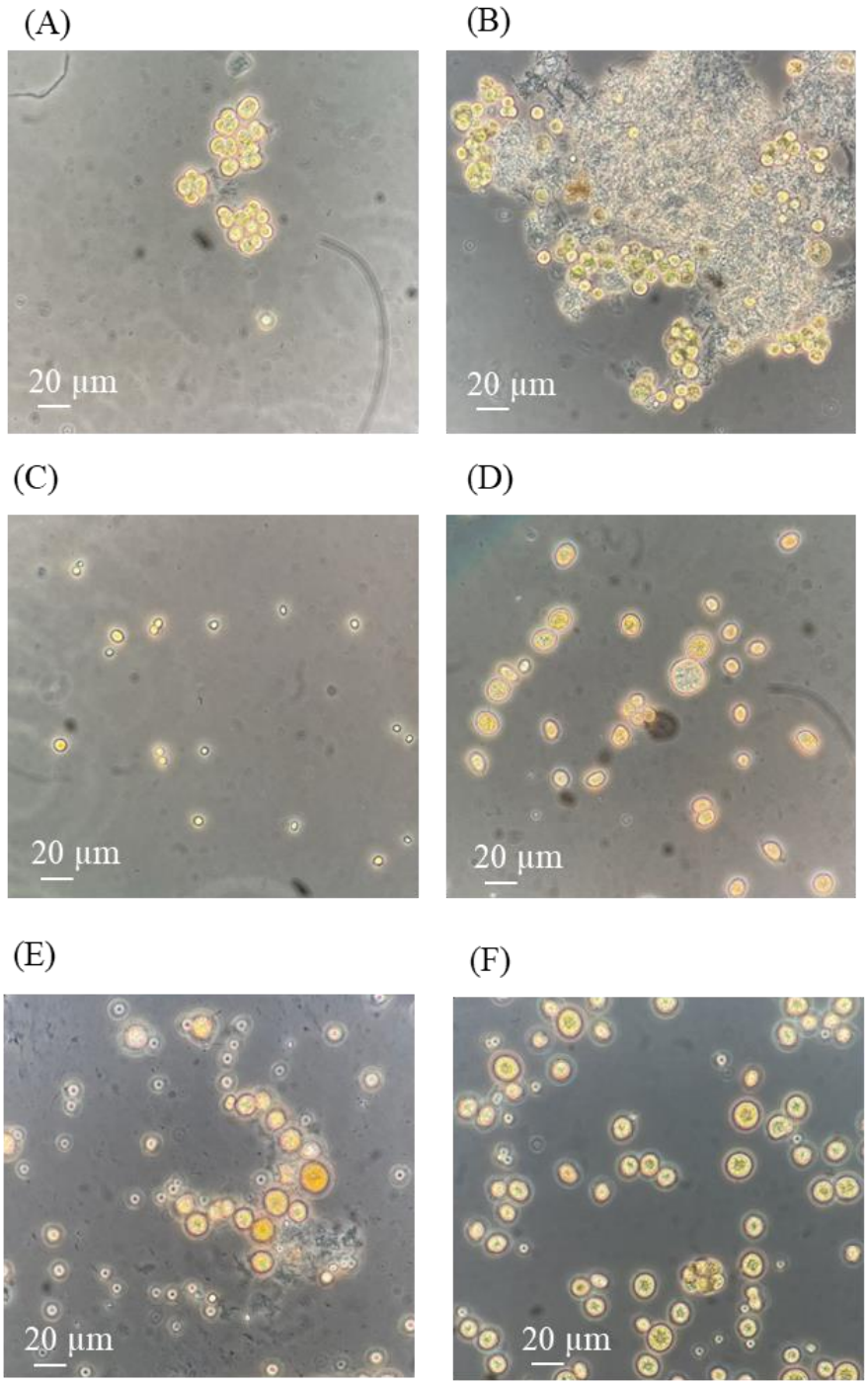


Fig. 13. Microscopic photo (magnification 40x) of *Neochloris* sp. with different medium and the concetration of $H_2S$ in biogas; [biogas0 ($CH_4$: 70%, $CO_2$: 30%)] pure cultivation of *Neochloris* sp. with MSM (A), microalgae-bacteria symbiotic consortia with 10% centrate with activated sludge (B), and the assay without microalgae (C) [biogas with low $H_2S$ (600 ppm)] pure cultivation of *Neochloris* sp. with 10% centrate (D), microalgae-bacteria symbiotic consortia with 10% centrate with activated sludge (E) [biogas with high $H_2S$ (5000 ppm)] 10% centrate with activated sludge (F).

### *4.4. Effect of different dilution ratios of centrate on cell proliferation when headspace is filled with biogas containing 600 ppm $H_2S$*

From the results of this study, *Neochloris* sp. reached the highest biomass yield under the condition of 10% diluted centrate with biogas containing 600 ppm $H_2S$. Centrates contain much ammonia, and it can lead to ammonia inhibition. Therefore, previous experiments used centrates diluted at 10% as a feedstock. However, the $CO_2$ present in biogas triggers acidification of pH in centrate, and *Neochloris* sp. grew as much as MSM and reached a steady state. Considering the practical application of coupling photosynthetic biogas upgrading with astaxanthin production, dilution of centrate needs water resources and leads to high costs. Hence, observing the effect of the amount of nitrogen on cell proliferation and astaxanthin accumulation is important to decide the optimum nitrogen concentration in centrate and supply rate for future application. Thus, this experiment examined the effect of different dilutions of centrates with biogas containing 600 ppm $H_2S$. Injection of biogas with 600 ppm $H_2S$ maintained initial pH of around 8 in all dilution conditions and resulted in the growth of *Neochloris* sp. in even 100% centrates (Fig. 14). All dilution conditions reached the steady state on day 5, and maximum TSS were 5.36±0.174 g $L^{-1}$ on day 9 (MSM), 6.19±0.409 g $L^{-1}$ on day6 (10%), 6.21±0.543 g $L^{-1}$ on day 5 (50%), 5.15±0.186 g $L^{-1}$ on day 6 (100%), respectively. There were no significant differences. After cells reached the steady state, cells density in 50% diluted centrate was suddenly decreased. On day 5, pH sharply increased from 9.15 to 12.0, and thus the proportion of ammonium ions converted to free ammonia. Therefore, cell density decreased due to ammonia inhibition. On the other hand, even though the pH in 10% diluted centrate increased, cell density did not decrease because ammonia in the centrates was already depleted after day 5. The assay conducted with 100% centrate maintained pH from 8.66 to 9.09 due to pH buffer effect, and results in avoiding decrease of the cell density. The bicarbonate buffer system is an acid-based homeostatic mechanism. The balance of carbonic acid ($H_2CO_3$), bicarbonate ion ($HCO_3^-$), and carbon dioxide ($CO_2$) regulates pH in the centrates. Carbon dioxide in the 100% centrate was not consumed up to all, and this remaining $CO_2$ in the bottles supports that the buffer effect occurred in this condition. Regarding decarbonization, MSM and 10% diluted centrate achieved 100% of $CO_2$ removal efficiency. $CO_2$ removal efficiencies in 50% and 10% diluted centrate were 99.9% and 94.5%, respectively. It is concluded that 100% centrate could be utilized for the cultivation of *Neochloris* sp. However, the starting date of astaxanthin induction differs due to the remaining nitrogen resources in the media. As shown in Fig. 15B, total nitrogen was depleted on day 4 under the conditions of 10% and 50% diluted centrate, and the color change of microalgae was detected on day 6 and 8, respectively. Total nitrogens in MSM and 100% centrate were 268±1.5 mg $L^{-1}$ and 305±7.2 mg $L^{-1}$, and this biomass changed its color on day 10 and 14.

Total carotenoids and astaxanthin were estimated using microalgae grown on day 10. Total carotenoids of 207.7±26.5 mg $g^{-1}$ in 100% was significantly higher than MSM of 84.2±3.82 mg $g^{-1}$, 10% of 29.4±2.84 mg $g^{-1}$, 50% of 32.6±4.09 mg $g^{-1}$ (Fig. 16A). Astaxanthin of 0.177% in 100% was also higher than MSM of 0.072%, 10% of 0.025, and 50% of 0.028%. As shown in Fig. 16B, the color of biomass in 10% diluted centrate was yellow on day 6, while the other conditions were still green. 50% diluted centrate changed the color of biomass on day 8. Even though 10% and 50% diluted centrate induced astaxanthin accumulation due to nitrogen deficiency, optical density at 750 in 50% decreased after the steady state (Fig. 14A). Dead cells were also observed in 10% and 50% from the microscopic observation. Thus, total carotenoids and astaxanthin might be lost in 10% and 50% diluted centrate. In this study, *Neochloris* sp. showed a higher accumulation of carotenoids and astaxanthin using MSM (nitrate-based) compared to 100% (ammonia-based). On the other hand, a previous study showed *Chlorella vulgaris* contained higher astaxanthin using nitrate-based media than ammonium-based media

(Simsek and Cetin, 2019). The influence of nitrogen-source on astaxanthin accumulation might be species dependents. Few results of astaxanthin production using *Neochloris* sp. were reported. Hence, future study needs to investigate the influence of nitrogen-source on an accumulation of carotenoids and astaxanthin with different species.

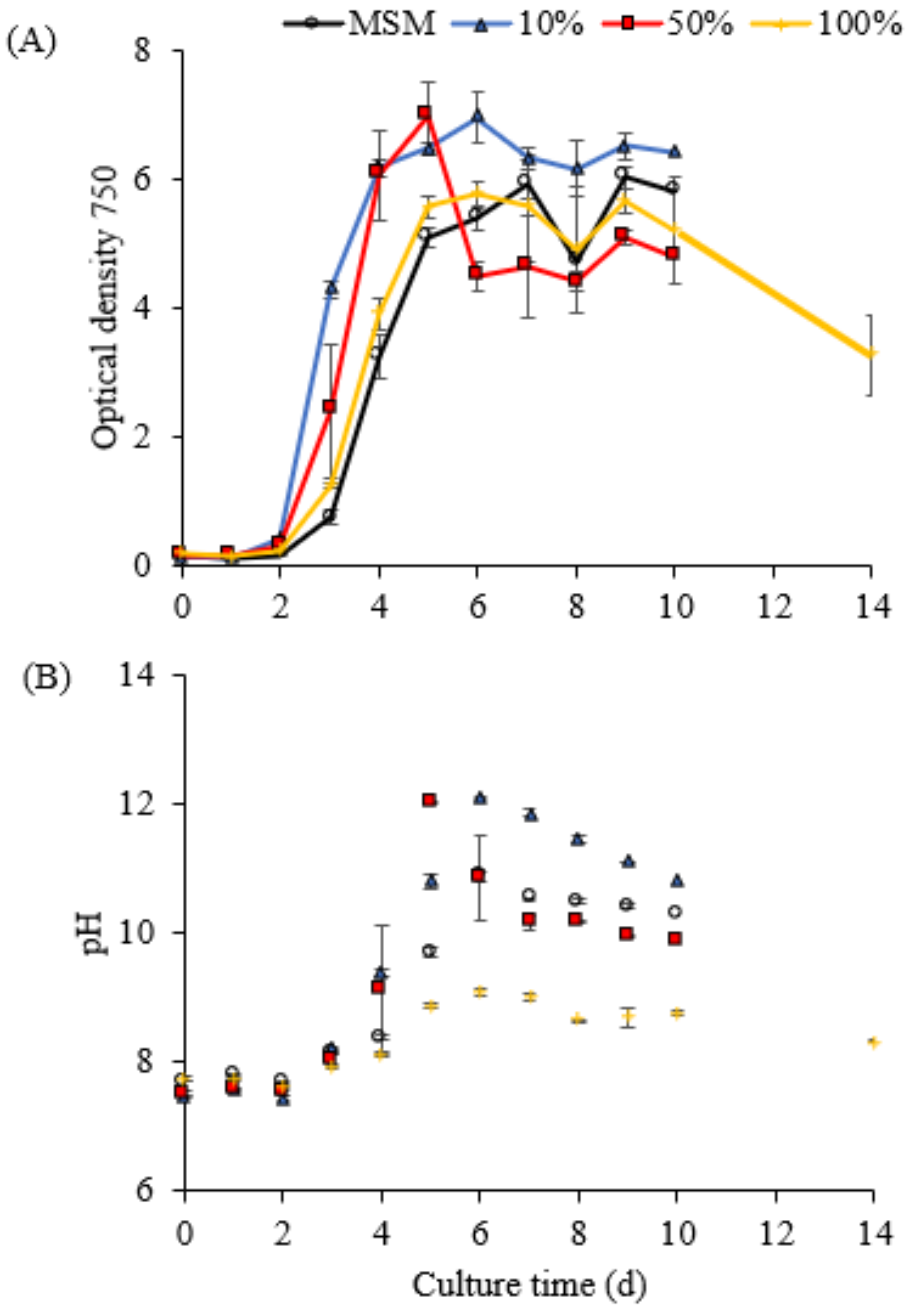


Fig. 14. Time course of the optical density at 750 nm (A) and pH (B) under different dilution conditions of centrate with biogas contained high $H_2S$ ($CH_4$: 65%, $CO_2$: 35%, $H_2S$: 600 ppm) in the headspace of the bottles.

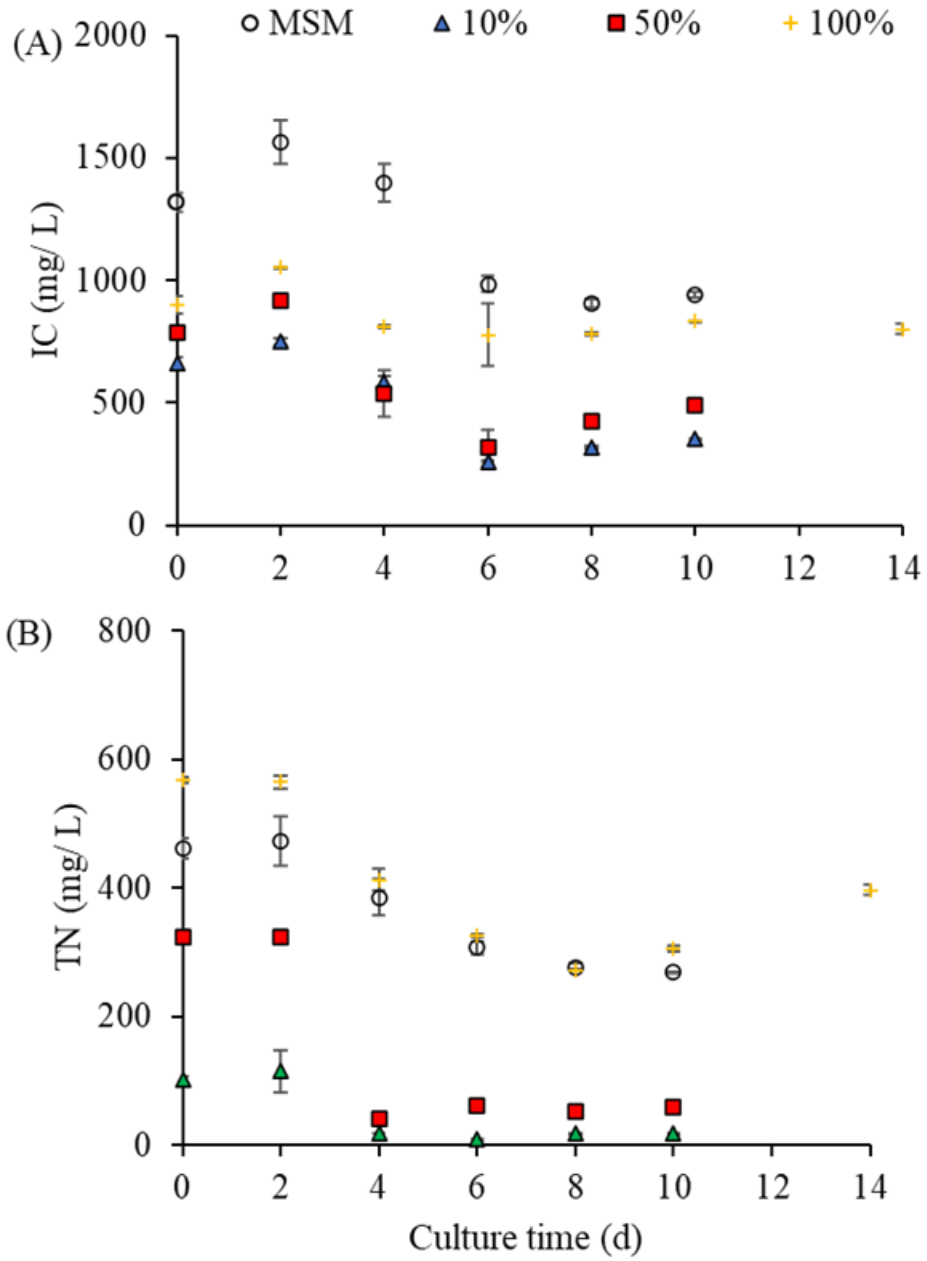


Fig. 15. Time course of total inorganic carbon (A) and total nitrogen (B) under different dilution conditions of centrate with biogas contained high $H_2S$ ($CH_4$: 65%, $CO_2$: 35%, $H_2S$: 600 ppm) in the headspace of the bottles.

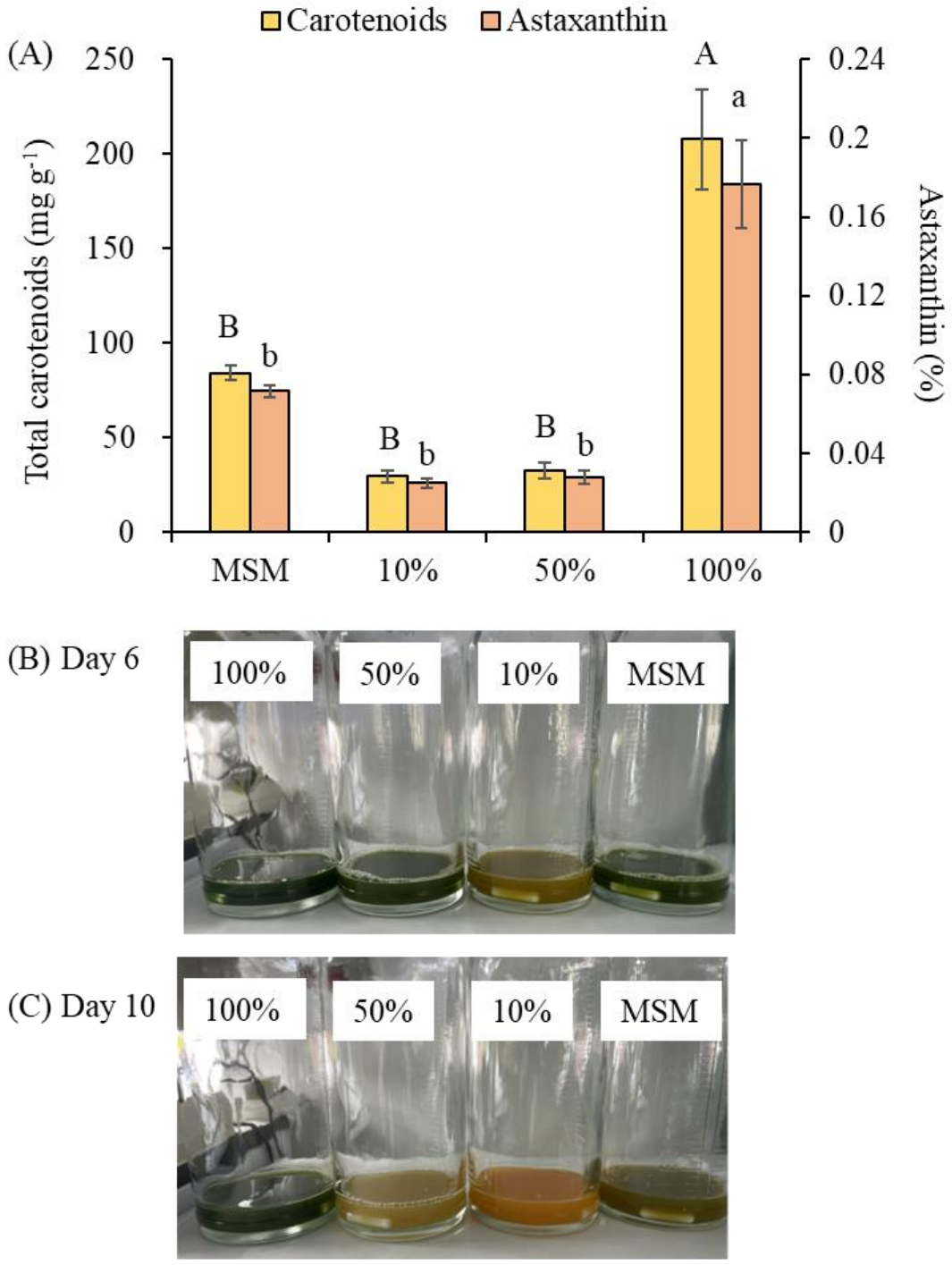


Fig. 16. Total carotenoids (mg $g^{-1}$) and astaxanthin (%) of *Neochloris* sp. on day 10. One-way ANOVA of variance followed by Tukey-Kramer test was used to determine the significance of the value ($p$<0.05). Photographs of the biomass on day 6 (B) and day10 (C).

### 4.5. *Comparison of biomass yield and astaxanthin yield with previous studies*

Table 3 shows comparison of biomass yield with other astaxanthin producers. TSS of 5.15±0.16 g $L^{-1}$ (100% centrate), 6.2±0.48 g $L^{-1}$ (50% diluted centrate), and 6.19±0.36~6.98±0.029 g $L^{-1}$ (10% diluted centrate) with biogas containing 600 ppm showed comparative with that of ~3.5 g $L^{-1}$ (Ip et al., 2004), 12.4 g $L^{-1}$ (Liu et al., 2012) using *Chlorella zofigiensis* and 2.28 g $L^{-1}$ using *H. pluvialis* (Kang et al., 2007). For photosynthetic biogas upgrading, biomass yield of 2.6±300 g $L^{-1}$ using *Mychonastes homosphaera* (Toledo-Cervantes et al., 2017b), and 0.4475 g $L^{-1}$ using *Leptolyngbya lagerheimii* (54%), *Chlorella vulgaris* (28%), *Parachlorella kessleri* (9%), *Tetradesmus obliquus* (5%), and *Mychonastes homosphaera* (2%) (Marin et al., 2018) were reported. From this comparison, this study indicated that *Neochloris* sp. achieved comparative or higher biomass yield as the same time as photosynthetic biogas upgrading, although these previous studies for photosynthetic biogas upgrading was conducted larger scale and continuous operation. Thus, future study needs to confirm the proof of concept using *Neochloris* sp. in large scale and continuous supply of biogas.

On a commercial scale, astaxanthin is typically produced using a two-way process (green and red inductive phase) to optimize culture conditions for growth and astaxanthin accumulation. On the other hand, photosynthetic biogas upgrading is commonly implemented in a bubble column for $CO_2$ and $H_2S$ scrubbing coupled to a HRAP for $CO_2$ fixation due to low operation cost and easy maintenance (Fig. 1). However, a recent study mentioned the economic benefit of flat panel photobioreactor for cultivation for high-value-added products simultaneously with biogas upgrading (Bose et al., 2019). Although a flat panel photobioreactor consumes more electricity than HRAP, it maintains high cell density and low contamination risk, so it is preferable for high-value-added compounds production that meets the local and global regulations for food safety. Hence, cultivation process containing supply rate of nutrient and biogas, and reactor configuration needs to be designed considering economic sustainability in future study.

Table 3 Comparison of biomass yield and astaxanthin yield with other species

| Algal strains | Cultivation mode | Culture time | Biomass yield (g $L^{-1}$) | Astaxanthin yield | References |
|---|---|---|---|---|---|
| **Astaxanthin producer** | | | | | |
| *Chlorella zofingiensis* | 100-mL mixtrophic culture | - | ~3.5 | 2.5 (mg $L^{-1}$) | Ip et al., 2004 |
| | 800-mL semi-continuous culture | 8 | 12.4 | 13.8 (mg $L^{-1}$) | Liu et al., 2012 |
| | - | - | - | 0.06-0.5 (%) | Zhang et al., 2016 |
| *Haematococcus pluvialis* | 130-mL batch cultivation | 18 | 2.28 | 77 (mg $L^{-1}$) | Kang et al., 2007 |
| | - | - | - | 5-6 (%) | Yang et al., 2016 |
| **Speceis for photosynthetic biogas upgrading** | | | | | |
| *Mychonastes homosphaera* | 180-L Indoor HRAP in continuous mode | - | 2.6 | - | Toledo-Cervante et al., 2017 |
| *Leptolyngbya lagerheimii* (54%), *Chlorella vulgaris* (28%), *Parachlorella kessleri* (9%), *Tetradesmus obliquus* (5%), *Mychonastes homosphaera* (2%) | 180-L Outdoor HRAP in continuous mode | - | 0.448 | - | Marin et al., 2018 |
| *Neochloris* sp. | 200-mL batch cultivation | 10 | 5.01~5.36 (MSM) | 0.072 (%) | This study |
| | | 14 | 5.15 (100%) | 0.025 (%) | |
| | | 10 | 6.2 (50%) | 0.028 (%) | |
| | | 10 | 6.19~6.98 (10%) | 0.177 (%) | |

*Astaxanthin yield (%) showed astaxanthin weight/ dry biomass weight.

## 5. Conclusions

This study demonstrated the feasibility of coupling photosynthetic biogas upgrading with high-added-value bioproduct synthesis. The astaxanthin producer, *Neochloris* sp. grew well with even 100% centrate and achieved 95% $CO_2$ removal efficiency with biogas containing 600 ppm $H_2S$. This result showed that biogas containing high concentration of $CO_2$ could control pH in the medium, and $NH_4^+$ in centrate was used for photosynthesis without inhibition by free ammonia. On the other hand, low concentrations of nitrogen are preferable to reduce the astaxanthin induction time. Addition of activated sludge aliquot was shown the effectiveness to remove the $CO_2$ present in biogas containing high $H_2S$ (5000 ppm). Interestingly, a concentration of 600 ppm $H_2S$ promoted the growth and showed almost two-fold higher TSS of 6.98±0.029 g $L^{-1}$ than biogas without $H_2S$ and with 5000 ppm $H_2S$. This value was higher than other strains for the astaxanthin production and photosynthetic biogas upgrading. Thus, photosynthetic biogas upgrading using *Neochloris* sp. can support the valorization of residual effluents such as digestate and biogas in the form of high added value pigments and biomass.

## 6. References

Arab News, 2021. NEOM, TRSDC to help boost Saudi aquaculture yield fivefold by 2030. https://www.arabnews.com/node/1989141/business-economy. (Accessed 10 July 2023).

Bose, A., O'Shea, R., Lin, R., Murphy, J.D., 2020. A perspective on novel cascading algal biomethane biorefinery systems. Bioresour. Technol. 304, 123027. https://doi.org/10.1016/j.biortech.2020.123027

Chekanov, K., Schastnaya, E., Solovchenko, A., Lobakova, E., 2017. Effects of CO2 enrichment on primary photochemistry, growth and astaxanthin accumulation in the chlorophyte *Haematococcus pluvialis*. J. Photochem. Photobiol. B Biol. 171, 58–66. https://doi.org/10.1016/j.jphotobiol.2017.04.028

Cheng, J., Wang, Z., Lu, H., Xu, J., He, Y., Cen, K., 2019. Hydrogen Sulfide Promotes Cell Division and Photosynthesis of *Nannochloropsis oceanica* with 15% Carbon Dioxide. ACS Sustain. Chem. Eng. 7, 16344–16354. https://doi.org/10.1021/acssuschemeng.9b03398

Cyanotech. 2013. Analysis of Natural Astaxanthin derived from *Haematococcus* Microalgae in Astaxanthin Oleoresin, Astaxanthin Gelcaps, Astaxanthin Beadles, and *Haematococcus* Biomass. https://www.cyanotech.com/pdfs/HPLC_Analysis_of_Natural_Astaxanthin_031513.pdf (Accessed 10 July 2023).

Eren, B., Tuncay Tanrıverdi, S., Aydın Köse, F., Özer, Ö., 2019. Antioxidant properties evaluation of topical astaxanthin formulations as anti-aging products. J. Cosmet. Dermatol. 18, 242–250. https://doi.org/10.1111/jocd.12665

Farruggia, C., Kim, M.B., Bae, M., Lee, Y., Pham, T.X., Yang, Y., Han, M.J., Park, Y.K., Lee, J.Y., 2018. Astaxanthin exerts anti-inflammatory and antioxidant effects in macrophages in NRF2-dependent and independent manners. J. Nutr. Biochem. 62, 202–209. https://doi.org/10.1016/j.jnutbio.2018.09.005

Florencio, F.J., Vega, J.M., 1983. Utilization of nitrate, nitrite and ammonium by *Chlamydomonas reinhardii* - Photoproduction of ammonium. Planta 158, 288–293. https://doi.org/10.1007/BF00397329

García-Malea, M.C., Gabriel Acién, F., Río, E. Del, Fernández, J.M., Cerón, M.C., Guerrero, M.G., Molina-Grima, E., 2009. Production of astaxanthin by *Haematococcus pluvialis*: Taking the one-step system outdoors. Biotechnol. Bioeng. 102, 651–657. https://doi.org/10.1002/bit.22076

Ip, P.F., Wong, K.H., Chen, F., 2004. Enhanced production of astaxanthin by the green microalga *Chlorella zofingiensis* in mixotrophic culture. Process Biochem. 39, 1761–1766. https://doi.org/10.1016/j.procbio.2003.08.003

Kang, C.D., Lee, J.S., Park, T.H., Sim, S.J., 2007. Complementary limiting factors of astaxanthin synthesis during photoautotrophic induction of *Haematococcus pluvialis*: C/N ratio and light intensity. Appl. Microbiol. Biotechnol. 74, 987–994. https://doi.org/10.1007/s00253-006-0759-x

Kang, C.D., An, J.Y., Park, T.H., Sim, S.J., 2006. Astaxanthin biosynthesis from simultaneous N and P uptake by the green alga *Haematococcus pluvialis* in primary-treated wastewater. Biochem. Eng. J. 31, 234–238. https://doi.org/10.1016/j.bej.2006.08.002

Kishimoto, Y., Yoshida, H., Kondo, K., 2016. Potential anti-atherosclerotic properties of astaxanthin. Mar. Drugs 14, 1–13. https://doi.org/10.3390/md14020035

Klatt, J.M., Haas, S., Yilmaz, P., de Beer, D., Polerecky, L., 2015. Hydrogen sulfide can inhibit and enhance oxygenic photosynthesis in a cyanobacterium from sulfidic springs. Environ. Microbiol. 17, 3301–3313. https://doi.org/10.1111/1462-2920.12791

Lisjak, M., Teklic, T., Wilson, I.D., Whiteman, M., Hancock, J.T., 2013. Hydrogen sulfide: Environmental factor or signaling molecule? Plant, Cell Environ. 36, 1607–1616. https://doi.org/10.1111/pce.12073

Liu, J., Huang, J., Jiang, Y., Chen, F., 2012. Molasses-based growth and production of oil and astaxanthin by *Chlorella zofingiensis*. Bioresour. Technol. 107, 393–398. https://doi.org/10.1016/j.biortech.2011.12.047

Malik, K.A., 1983. A modified method for the cultivation of phototrophic bacteria. J. Microbiol. Methods 1, 343–352. https://doi.org/10.1016/0167-7012(83)90011- 8

Marín, D., Posadas, E., Cano, P., Pérez, V., Blanco, S., Lebrero, R., Muñoz, R., 2018. Seasonal variation of biogas upgrading coupled with digestate treatment in an outdoors pilot scale algal-bacterial photobioreactor. Bioresour. Technol. 263, 58–66. https://doi.org/10.1016/j.biortech.2018.04.117

Markou, G., Vandamme, D., Muylaert, K., 2014. Microalgal and cyanobacterial cultivation: The supply of nutrients. Water Res. 65, 186–202. https://doi.org/10.1016/j.watres.2014.07.025

Meier, L., Stará, D., Bartacek, J., Jeison, D., 2018. Removal of H2S by a continuous microalgae-based photosynthetic biogas upgrading process. Process Saf. Environ. Prot. 119, 65–68. https://doi.org/10.1016/j.psep.2018.07.014

Nagarajan, D., Lee, D.J., Chang, J.S., 2019. Integration of anaerobic digestion and microalgal cultivation for digestate bioremediation and biogas upgrading. Bioresour. Technol. 290, 121804. https://doi.org/10.1016/j.biortech.2019.121804

Nisar, N., Li, L., Lu, S., Khin, N.C., Pogson, B.J., 2015. Carotenoid metabolism in plants. Mol. Plant 8, 68–82. https://doi.org/10.1016/j.molp.2014.12.007

Ohki, K., Yamada, K., Kamiya, M., Yoshikawa, S., 2012. Morphological, phylogenetic and physiological studies of pico-cyanobacteria isolated from the halocline of a saline Meromictic Lake, Lake Suigetsu, Japan. Microbes Environ. 27, 171–178. https://doi.org/10.1264/jsme2.ME11329

Orosa, M., Valero, J.F., Herrero, C., Abalde, J., 2001. Comparison of the accumulation of astaxanthin in *Haematococcus pluvialis* and other green microalgae under N-starvation and high light conditions. Biotechnol. Lett. 23, 1079–1085. https://doi.org/10.1023/A:1010510508384

Patel, A.K., Tambat, V.S., Chen, C.W., Chauhan, A.S., Kumar, P., Vadrale, A.P., Huang, C.Y., Dong, C. Di, Singhania, R.R., 2022. Recent advancements in astaxanthin production from microalgae: A review. Bioresour. Technol. 364, 128030. https://doi.org/10.1016/j.biortech.2022.128030

Perez-Garcia, O., Escalante, F.M.E., de-Bashan, L.E., Bashan, Y., 2011. Heterotrophic cultures of microalgae: Metabolism and potential products. Water Res. 45, 11–36. https://doi.org/10.1016/j.watres.2010.08.037

Posadas, E., Morales, M. del M., Gomez, C., Acién, F.G., Muñoz, R., 2015. Influence of pH and CO2 source on the performance of microalgae-based secondary domestic wastewater treatment in outdoors pilot raceways. Chem. Eng. J. 265, 239–248. https://doi.org/10.1016/j.cej.2014.12.059

Ranjbar, R., Inoue, R., Shiraishi, H., Katsuda, T., Katoh, S., 2008. High efficiency production of astaxanthin by autotrophic cultivation of *Haematococcus pluvialis* in a bubble column photobioreactor. Biochem. Eng. J. 39, 575–580. https://doi.org/10.1016/j.bej.2007.11.010

Sekine, M., Yoshida, A., Kishi, M., Furuya, K., Toda, T., 2023. Free ammonia tolerance of cyanobacteria depends on intracellular pH. Biocatal. Agric. Biotechnol. 47, 102562. https://doi.org/10.1016/j.bcab.2022.102562

Simsek, G. K., & Cetin, A.K., 2019. Effect of Nitrogen Sources on Growth, Protein, Total Lipid Amount and Pigment Content in *Chlorella Vulgaris*. Environ. Bull. 28, 3065–72.

Song, X., Wang, L., Li, X., Chen, Z., Liang, G., Leng, X., 2017. Dietary astaxanthin improved the body pigmentation and antioxidant function, but not the growth of discus fish (*Symphysodon* spp.). Aquac. Res. 48, 1359–1367. https://doi.org/10.1111/are.13200

Toledo-Cervantes, A., Estrada, J.M., Lebrero, R., Muñoz, R., 2017a. A comparative analysis of biogas upgrading technologies: Photosynthetic vs physical/chemical processes. Algal Res. 25, 237–243. https://doi.org/10.1016/j.algal.2017.05.006

Toledo-Cervantes, A., Madrid-Chirinos, C., Cantera, S., Lebrero, R., Muñoz, R., 2017b. Influence of the gas-liquid flow configuration in the absorption column on photosynthetic biogas upgrading in algal-bacterial photobioreactors. Bioresour. Technol. 225, 336–342. https://doi.org/10.1016/j.biortech.2016.11.087

Wan, M., Zhang, J., Hou, D., Fan, J., Li, Y., Huang, J., Wang, J., 2014. The effect of temperature on cell growth and astaxanthin accumulation of *Haematococcus pluvialis* during a light-dark cyclic cultivation. Bioresour. Technol. 167, 276–283. https://doi.org/10.1016/j.biortech.2014.06.030

Wu, Y.H., Yang, J., Hu, H.Y., Yu, Y., 2013. Lipid-rich microalgal biomass production and nutrient removal by *Haematococcus pluvialis* in domestic secondary effluent. Ecol. Eng. 60, 155–159. https://doi.org/10.1016/j.ecoleng.2013.07.066

Yang, Z., Cheng, J., Li, K., Zhou, J., Cen, K., 2016. Optimizing gas transfer to improve growth rate of *Haematococcus pluvialis* in a raceway pond with chute and oscillating baffles, Bioresour. Technol. 214 276–283, https://doi.org/10.1016/J.BIORTECH.2016.04.107.

Ytrestøyl, T., Struksnæs, G., Rørvik, K.A., Koppe, W., Bjerkeng, B., 2006. Astaxanthin digestibility as affected by ration levels for Atlantic salmon, Salmo salar. Aquaculture 261, 215–224. https://doi.org/10.1016/j.aquaculture.2006.06.046

Yu, C., Wang, H.P., Yu, X., 2022. The associative induction of succinic acid and hydrogen sulfide for high-producing biomass, astaxanthin and lipids in *Haematococcus pluvialis*. Bioresour. Technol. 358, 127397. https://doi.org/10.1016/j.biortech.2022.127397

Zhang, B.Y., Geng, Y.H., Li, Z.K., Hu, H.J., Li, Y.G., 2009. Production of astaxanthin from *Haematococcus* in open pond by two-stage growth one-step process. Aquaculture 295, 275–281. https://doi.org/10.1016/j.aquaculture.2009.06.043

Zhang, W., Wang, Junfeng, Wang, Jialin, Liu, T., 2014. Attached cultivation of *Haematococcus pluvialis* for astaxanthin production. Bioresour. Technol. 158, 329–335. https://doi.org/10.1016/j.biortech.2014.02.044

Zhang, Z., Sun, D., Mao, X., Liu, J., Chen, F., 2016. The crosstalk between astaxanthin, fatty acids and reactive oxygen species in heterotrophic *Chlorella zofingiensis*, Algal Res. 19 178–183, https://doi.org/10.1016/j.algal.2016.08.015.

# 8 Appendix

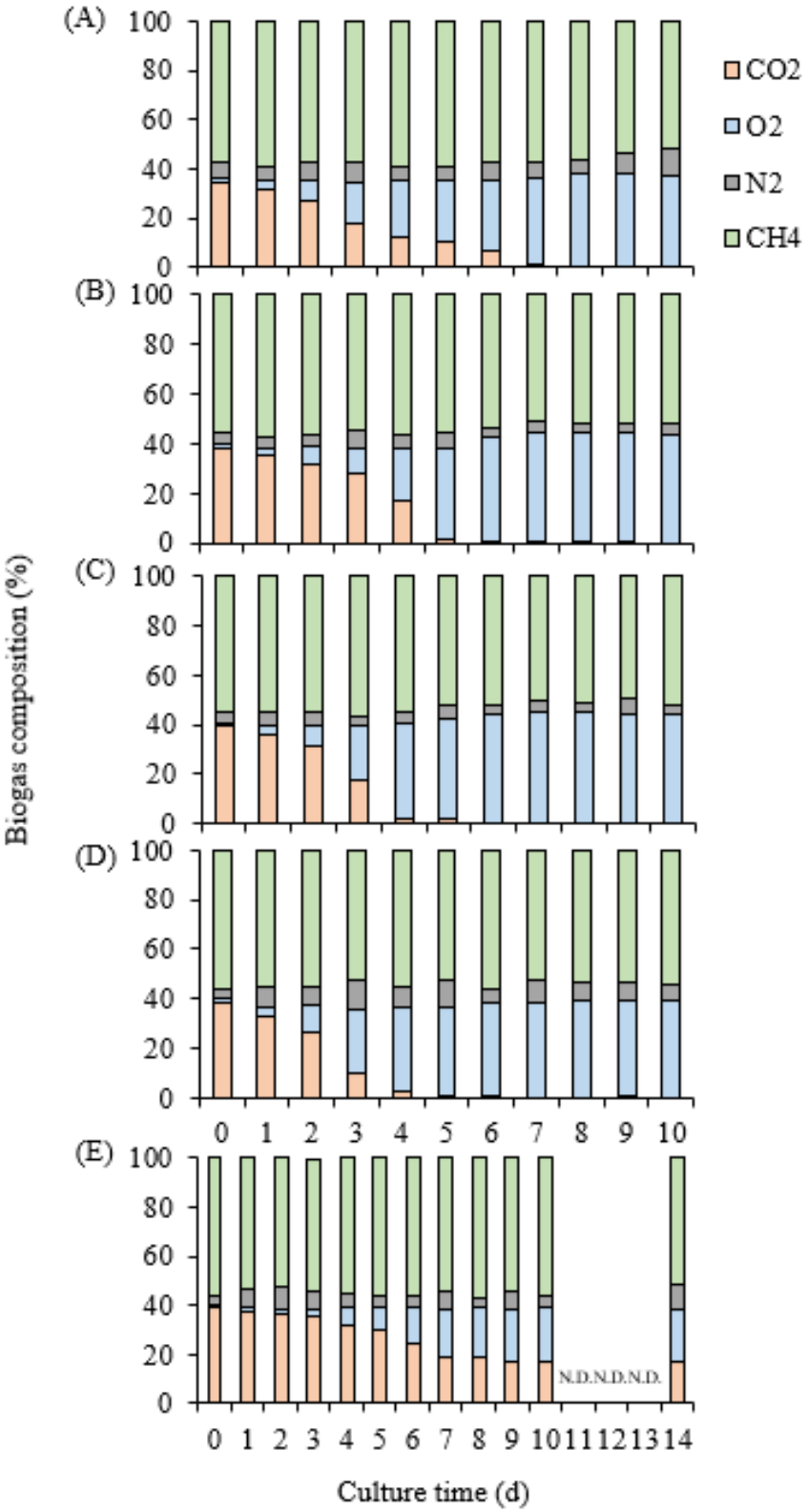


Fig. Time course of the gas composition in the headspace of the bottles injected biogas0 ($CH_4$: 70%, $CO_2$: 30%) with different medium conditions; MSM (A), centrate diluted at 10% (B), that of initial pH 7 (C), that with activated sludge (D), and that with activated sludge uninoculated microalgae (E).

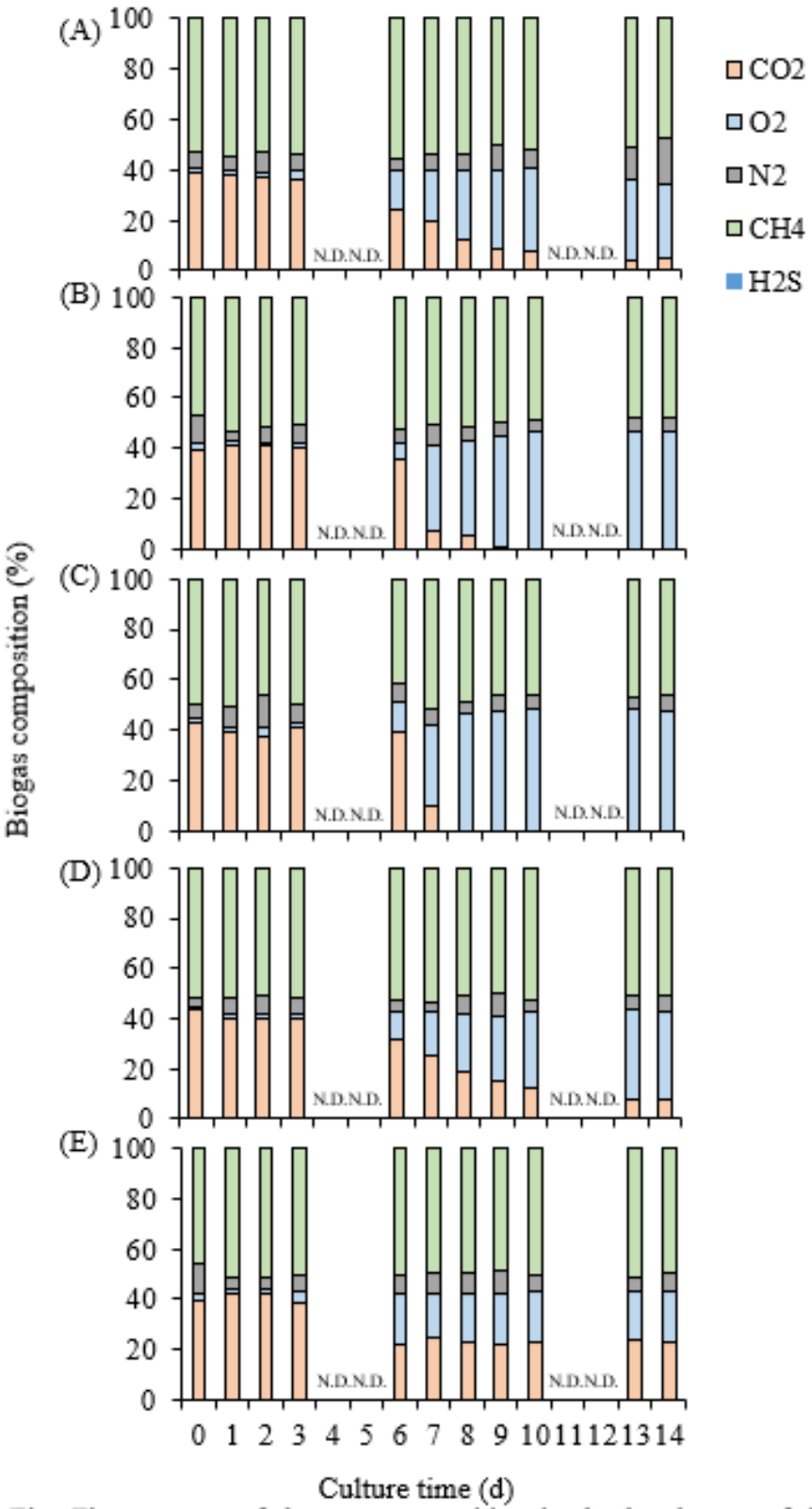


Fig. Time course of the gas composition in the headspace of the bottles injected biogas contained low $H_2S$ ($CH_4$: 65%, $CO_2$: 35%, $H_2S$: 600 ppm) under different medium conditions; MSM (A), centrate diluted at 10% (B), that of initial pH 7 (C), that with activated sludge (D), and that with activated sludge uninoculated microalgae (E).

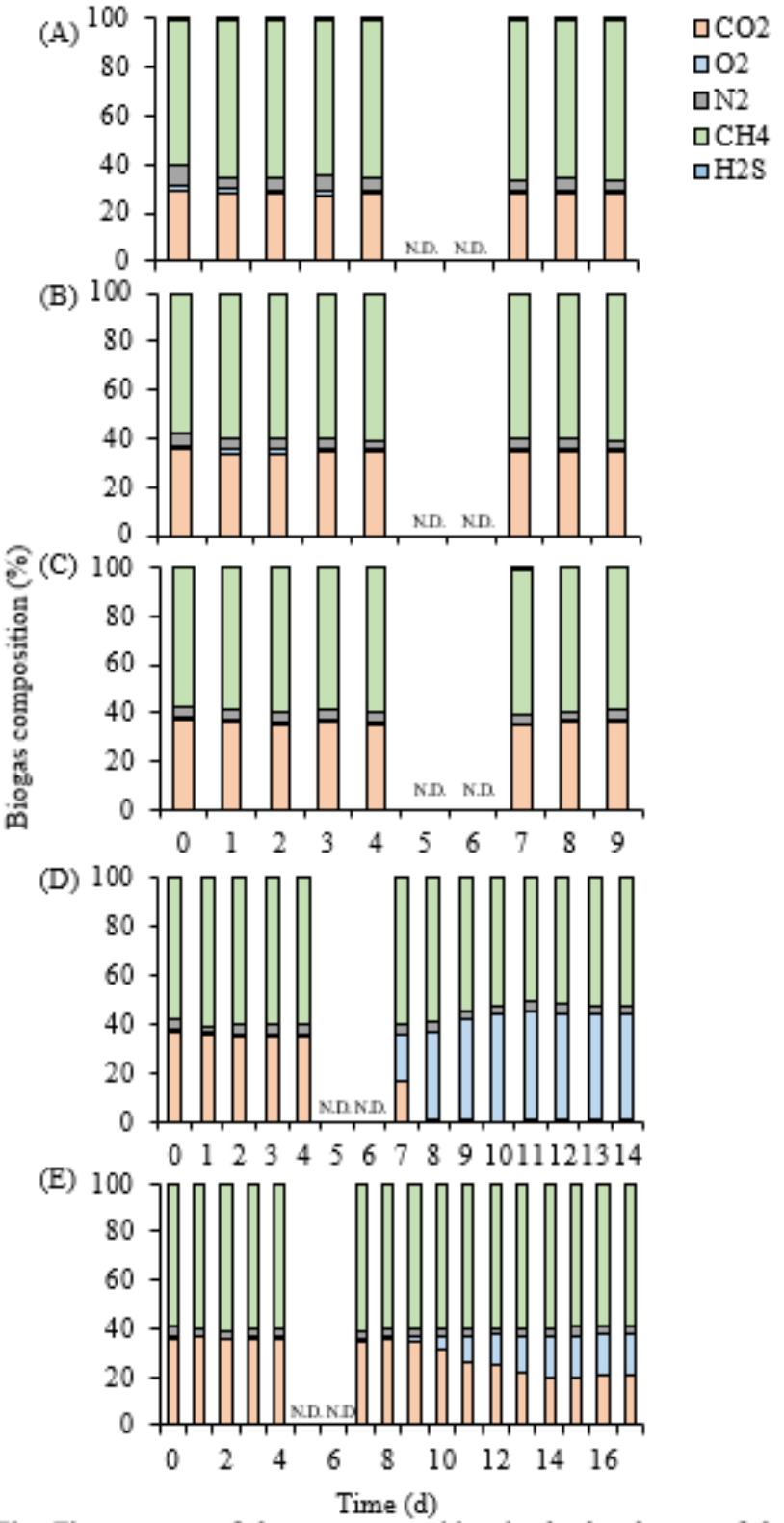


Fig. Time course of the gas composition in the headspace of the bottles injected biogas contained high $H_2S$ ($CH_4$: 70%, $CO_2$: 29.5%, $H_2S$: 5000 ppm) under different medium conditions; MSM (A), centrate diluted at 10% (B), that of initial pH 7 (C), that with activated sludge (D), and that with activated sludge uninoculated microalgae (E).

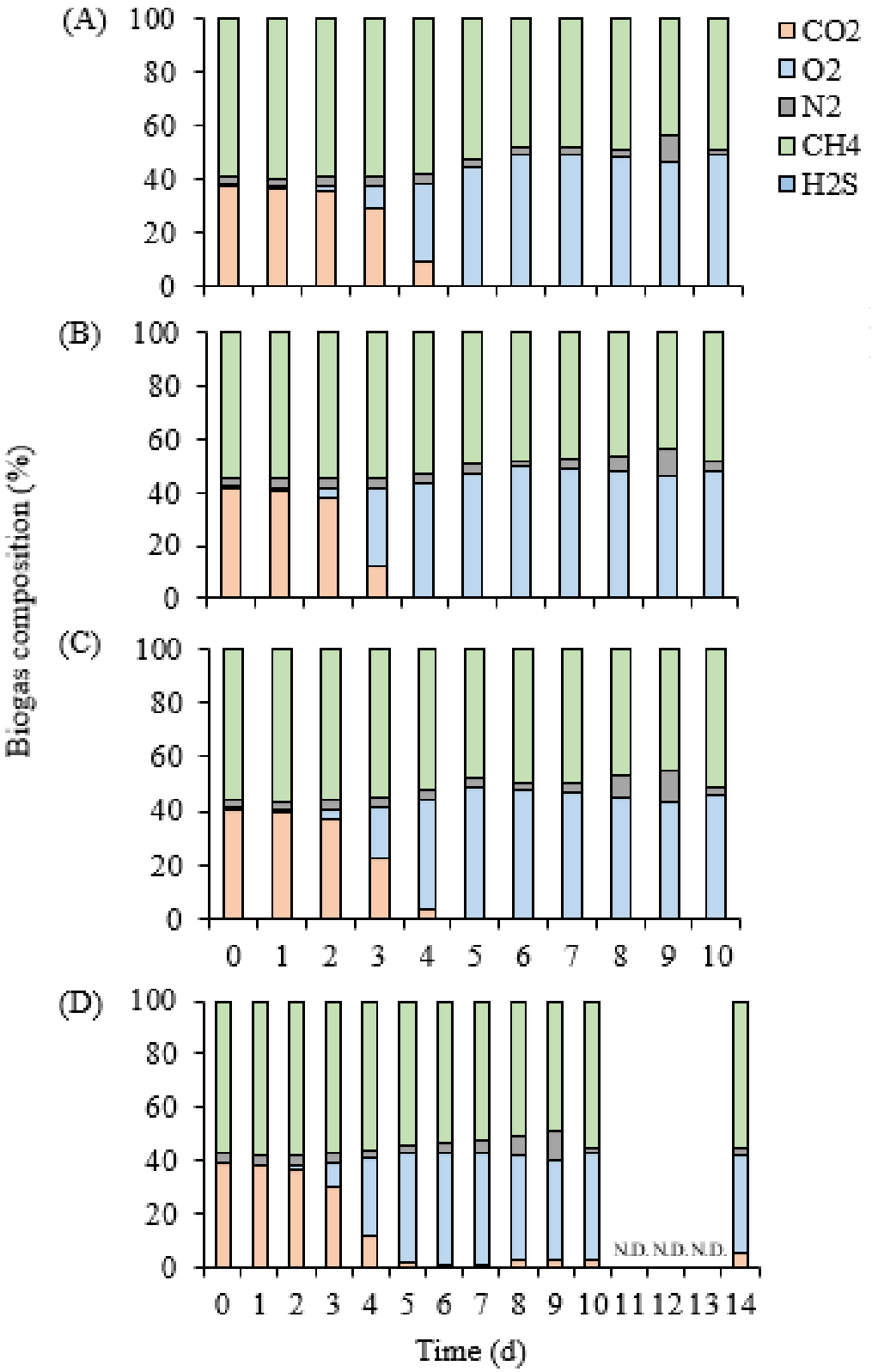


Fig. Time course of the gas composition in the headspace of the bottles injected biogas contained low $H_2S$ ($CH_4$: 65%, $CO_2$: 35%, $H_2S$: 600 ppm) under different medium conditions; MSM (A), centrate diluted at 10% (B), 50% (C), and 100% (D).